

Attachment 1

CHLE-005:

Determination of the Initial Pool Chemistry for the CHLE Test,  
Revision 2

## PROJECT DOCUMENTATION COVER PAGE

Document No: CHLE-005	Revision: 2	Page 1 of 47
Title: Determination of the initial pool chemistry for the CHLE test		
Project: Corrosion/Head Loss Experiment (CHLE) Program		Date: 2/18/2014
Client: South Texas Project Nuclear Operating Company		

**Summary/Purpose of Analysis or Calculation:**

The purpose of this calculation is to determine the chemical constituents and associated concentrations in the Corrosion/Head Loss Experiment (CHLE) bulk solution before the addition of corrosion or dissolution products. A review of 2 years of historical analyte data obtained from STP was performed to identify chemical constituents that may be included in the CHLE tests. Upon identification of the chemical constituents to be included, a maximum, minimum, and average concentrations were determined for each constituent in the three sources of solution: the refueling water storage tank, the reactant cooling system, and the safety injection accumulators. The chemical constituent concentrations and solution volume of these three sources were used to determine the final mass of the chemical constituents. The final mass of the chemical constituents and the total volume of solution as a result of a Loss-of-Coolant Accident (LOCA) were used to calculate minimum, maximum, and average chemical constituent concentrations which will be used in the CHLE test matrix. The average concentrations of the chemical constituents will be used for the 30 day tank tests bulk solution. The minimum and maximum chemical constituent concentrations will be included within the bounds of the laboratory tests.

The analysis of STP pool chemistry in this document is based on information that was available at the time this document was prepared. Where final information was not available, values for chemical concentrations used in CHLE tests will be identified in the individual test plan documents.

Role:	Name:	Signature:	Date:
Prepared:	Janet Leavitt	< signed electronically >	8/13/2012
Reviewed:	Kerry Howe	< signed electronically >	8/13/2012
Oversight:	Zahra Mohaghegh	< signed electronically >	2/11/2014
Approved:	Ernie Kee	< signed electronically >	2/18/2014

Revision	Date	Description
0	3/12/2012	Draft document for internal review
1	8/13/2012	Includes revisions from internal review
2	2/18/2014	Review for NRC submittal

## Table of Contents

Table of Contents .....	2
List of Figures .....	3
List of Tables .....	4
Definitions and Acronyms.....	5
1 Purpose .....	6
2 Methodology .....	6
2.1 Statistics .....	7
2.2 pH Profile as a Function of TSP Dissolution and Break Type .....	8
2.3 Acid Generation Due to Irradiation.....	8
3 Design Input and Analyses.....	9
3.1 Containment Pool Volume .....	9
3.2 Trisodium Phosphate .....	10
3.3 Boron.....	10
3.4 Silicon.....	25
3.5 Lithium .....	31
3.5.1 RCS Lithium Concentration.....	31
3.6 Zinc.....	32
3.6.1 RCS Zinc Concentration .....	32
3.7 Environmental Contribution (O <sub>2</sub> and CO <sub>2</sub> ).....	33
3.7.1 Oxygen.....	33
3.8 Impurities .....	36
3.8.1 Impurities .....	36
3.9 Pool pH.....	42
3.10 Acid Generation Due to Irradiation .....	44
4 CHLE Pool Chemistry.....	46
5 Conclusion.....	46
6 References .....	47

## List of Figures

Figure 1: Boron concentration for Unit 1 and 2 RCS as a function of time.....	12
Figure 2: RCS 1 Boron histogram. ....	12
Figure 3: RCS 1 Boron relative cumulative frequency graph. ....	13
Figure 4: RCS 2 Boron histogram. ....	14
Figure 5: RCS 2 Boron relative cumulative frequency graph. ....	15
Figure 6: Boron concentration in Unit 1 and Unit 2 RWST as a function of time. ....	16
Figure 7: Probability distribution function of RWST 1 Boron concentration. The blue line is the Johnson fit and the green line is the normal fit. ....	16
Figure 8: Probability distribution function of RWST 2 Boron concentration. The blue line is the Johnson fit and the green line is the normal fit. ....	17
Figure 9: Boron concentration of Accumulators as a function of time. ....	18
Figure 10: Accumulator 1A Boron histogram. ....	19
Figure 11: Accumulator 1A Boron relative cumulative frequency graph. ....	20
Figure 12: Probability distribution function of Accumulator 1B Boron concentration. The blue line is the Johnson fit and the green line is the normal fit. ....	20
Figure 13: Probability distribution function of Accumulator 1C Boron concentration. The blue line is the Johnson fit and the green line is the normal fit. ....	21
Figure 14: Probability distribution function of Accumulator 2A Boron concentration. The blue line is the Johnson fit and the green line is the normal fit. ....	22
Figure 15: Probability distribution function of Accumulator 2B Boron concentration. The blue line is the Johnson fit and the green line is the normal fit. ....	23
Figure 16: Probability distribution function of Accumulator 2C Boron concentration. The blue line is the Johnson fit and the green line is the normal fit. ....	24
Figure 17: Silicon as silica dioxide concentration in Unit 1 and Unit 2 RCS as a function of time. ....	26
Figure 18: RCS 1 Silica histogram. ....	27
Figure 19: RCS 2 Silica histogram. ....	28
Figure 20: Silicon as silica dioxide concentration in Units 1 and 2 RWST as a function of time. ....	29
Figure 21: RWST 1 Silica histogram. ....	29
Figure 22: RWST 2 silica histogram. ....	30
Figure 23: Lithium concentration in Unit 1 and Unit 2 RCS as a function of time. ....	32
Figure 24: Zinc concentration in Unit 1 and 2 RCS as a function of time. ....	33
Figure 25: Oxygen concentration in Unit 1 and Unit 2 RCS as a function of time. ....	34
Figure 26: Decrease in oxygen concentration as a function of temperature. ....	34
Figure 27: Magnesium concentration in Unit 1 and Unit 2 RCS as a function of time. ....	36
Figure 28: Aluminum concentration in Unit 1 and Unit 2 RCS as a function of time. ....	37
Figure 29: Sulfate concentration in Unit 1 and Unit 2 RCS as a function of time. ....	37
Figure 30: Fluoride concentration in Unit 1 and Unit 2 RCS as a function of time. ....	38
Figure 31: Chloride concentration in Unit 1 and Unit 2 RCS as a function of time. ....	38
Figure 32: Iron concentration in Unit 1 and Unit 2 RCS as a function of time. ....	39
Figure 33: Copper concentration in Unit 1 RCS as a function of time. ....	39

Figure 34: Nickel concentration in Unit 1 and Unit 2 RCS as a function of time. .... 40  
 Figure 35: Calcium concentration in Unit 1 and Unit 2 RCS as a function of time. .... 40  
 Figure 36: Magnesium concentration in Unit 1 and Unit 2 RWST as a function of time. .... 41  
 Figure 37: Aluminum concentration in Unit 1 and Unit 2 RWST as a function of time. .... 41  
 Figure 38: Iron concentration in Unit 1 RWST as a function of time. .... 42  
 Figure 39: Calcium concentration in Unit 1 and Unit 2 RWST as a function of time. .... 42  
 Figure 40: Aluminum solubility in borated buffered water. .... 44  
 Figure 41: Generation of strong acid following a LOCA ..... 45  
 Figure 42: Decrease in pool solution pH as a result of acid generation, using an initial pH of 7 as a basis  
 for comparison..... 45

**List of Tables**

Table 1: Design basis containment pool volume as a function of LOCA type [8]. .... 9  
 Table 2: “Best Estimate” Operating containment pool volume as a function of LOCA type [1]. .... 9  
 Table 3: Design basis Boron concentration ranges for contributing sources. .... 11  
 Table 4: Operating Boron concentration ranges for contributing sources..... 11  
 Table 5: Statistical RCS 1 data (Figure 2)..... 13  
 Table 6: Statistical RCS 2 data (Figure 4)..... 14  
 Table 7: Summary of Boron concentrations. .... 15  
 Table 8: Probability distribution statistics for RWST 1 Boron concentrations..... 17  
 Table 9: Probability distribution statistics for RWST 2 Boron concentrations..... 17  
 Table 10: Statistical results from the Boron concentration analyses of the RWST. .... 18  
 Table 11: Statistics for Accumulator 1A (Figure 10)..... 19  
 Table 12: Probability distribution function for Accumulator 1B Boron concentrations..... 21  
 Table 13: Probability distribution function for Accumulator 1C Boron concentrations..... 21  
 Table 14: Probability distribution statistics for Accumulator 2A Boron concentrations. .... 22  
 Table 15: Probability distribution statistics for Accumulator 2B Boron concentrations. .... 23  
 Table 16: Probability distribution statistics for Accumulator 2C Boron concentrations. .... 24  
 Table 17: Summary of accumulator concentration ranges..... 25  
 Table 18: Boron concentration used to determine the concentration in the 30-day CHLE tests. .... 25  
 Table 19: Boron concentrations to be investigated in the CHLE tests..... 25  
 Table 20: Statistics for RCS 1 Silica (Figure 18). .... 27  
 Table 21: Statistics for RCS 2 Silica (Figure 19). .... 28  
 Table 22: Statistics for RWST 1 Silica (Figure 21). .... 30  
 Table 23: Statistics for RWST 2 (Figure 22). .... 30  
 Table 24: Results associated with Silica histogram..... 31  
 Table 25: LBLOCA and MBLOCA concentration of Boron and Lithium in RCS. .... 32  
 Table 26: pH of the 30 Day test using the largest TSP concentration. .... 43  
 Table 27: Chemical conditions to be covered by the CHLE analyses. .... 46  
 Table 28: Acid addition to CHLE test..... 46

## Definitions and Acronyms

RCB	Reactor Containment Building
RCS	Reactant Cooling System
RWST	Refueling Water Storage Tank
SI	Safety Injection
SFP	Spent Fuel Pool
RMWST	Reactor Makeup Water Storage Tank
BAT	Boric Acid Tank
BARS	Boric Acid Recovery System

## 1 Purpose

The purpose of this calculation is to determine the chemical constituents and associated concentrations in the Chemical Head Loss Experiment (CHLE) bulk solution before the addition of corrosion or dissolution products. These values are important in conducting a risk informed approach in evaluation of potential safety issues as a result of a Loss of Coolant Accident (LOCA). The chemical constituent and associated concentrations of the post-LOCA reactor containment building (RCB) pool solution are necessary to determine the initial pool chemistry to predict the subsequent solution chemistry resulting from dissolution and corrosion of materials. A potential exists for the interaction of the pool chemistry and materials in containment to produce chemical precipitates that may negatively influence head loss across the sump strainer; possibly resulting in failure of the Emergency Core Cooling System (ECCS). An accurate value of total chemical constituent masses and containment pool volume determined from the various sources of solution will allow the CHLE analyses to investigate the most probable pool chemistry of a LOCA. This approach will determine a more realistic consequence of chemical reaction due to LOCA conditions on head loss across the sump strainer of the ECCS as compared to that determined using the deterministic approach.

To accomplish the task, two years of historical analyte data obtained from STP was reviewed to identify chemical constituents and associated concentrations that will be included in the CHLE tests. A maximum, minimum, and average concentration for the identified constituents were determined for each of the three sources of solution: the refueling water storage tank (RWST), the reactant cooling system (RCS), and the safety injection accumulators (accumulators). The chemical constituent concentrations and solution volume of each of these three sources [1] were used to determine the final mass of the chemical constituents for a post-LOCA pool solution. The average concentrations of the chemical constituents determined the 30 day CHLE tank tests bulk solution makeup. The minimum and maximum chemical constituent concentrations will be included within the bounds of the CHLE laboratory tests.

## 2 Methodology

The chemical constituents of the initial containment pool solution following a LOCA are variable because the final pool volume and chemical constituent concentrations are determined from three possible sources of solution. Each source of solution has a range of chemical constituents with associated concentrations and different solution volumes. For LBLOCA and MBLOCA, the final pool volume and chemistry is a combination of three sources of solution as follows: RWST (~80 % water mass), RCS (~16% water mass), and accumulators (~4% water mass) [1]. For a SBLOCA, the final pool volume is only a combination of two solution sources, the RWST (~85 % water mass) and the RCS (~15% water mass)[1].

Each source of solution is monitored for specific chemical constituents or analytes of interest and the sampling frequency for each analyte is variable. The type of analyte monitored and the frequency of monitoring is determined by the operational uses of the solution sources. The RCS and RWST are monitored for multiple chemical constituents, while the accumulators are only monitored for boron concentration. The solution in the accumulators are not monitored as closely as the other sources

because they are filled using the RWST solution. While the accumulators are charged from the RWST, they only have the same chemical make up at the point of recharge. The RWST solution is used during outages resulting in a hydraulic connection to the spent fuel pool (SFP). This connection results in other chemical constituents such as silicon to become part of the RWST chemistry.

Two years of historical data for aqueous chemical constituent concentrations in the various sources of solution at STP were collected and reviewed. Before the historical data was analyzed, data reflective of shut down operations was removed. The analyses of data obtained from normal operating conditions was used to identify which monitored chemical constituents would be eliminated and which would be included in the CHLE analyses. For the chemical constituents to be included in the CHLE analyses, the respective minimum, maximum, and average concentrations from each source of solution were determined using one of the three methods described below.

## 2.1 Statistics

The procedure used to determine a valid mathematical representation of a random variable given its sample of observed values. In statistics this procedure is known as a fitting procedure and typically consists of three steps:

1. Choose families of distributions to fit
2. Estimate distribution parameters for each family from step 1
3. Test the quality of the fit using quality of the fit statistics

It was decided to limit attention to the following three families of distributions - Normal, Lognormal and Johnson. The use of the Normal and Lognormal distributions is a standard practice. The Johnson distribution is known for its ability to model a wide variety of skewness and kurtosis combinations, so it was also used in the analyses to allow for greater flexibility of the fitting results.

Parameter estimation for the Normal and Lognormal distributions was done using Maximum Likelihood Estimation (MLE) procedure. If  $x_1, x_2, \dots, x_n$  is a sample then MLE for the Normal and Lognormal distributions are given by

- Normal:  $\hat{\mu} = \sum_{i=1}^n x_i / n, \hat{\sigma}^2 = \sum_{i=1}^n [x_i - \hat{\mu}]^2 / n$
- Lognormal:  $\hat{\mu} = \sum_{i=1}^n \ln(x_i) / n, \hat{\sigma}^2 = \sum_{i=1}^n [\ln(x_i) - \hat{\mu}]^2 / n$

For the Johnson distribution, numerical algorithms have to be used to estimate its parameters. The algorithm used in this analyses was proposed by Wheeler [2] and uses fifth order statistics to perform the fit.



The quality of fit was done using the two-sample Kolmogorov-Smirnov statistics (KS-statistics), where the first sample is the data used for the fitting and the second sample is data generated from the fitted distribution[3]. KS-statistic computes a distance between the empirical cumulative distribution functions of two samples, which is then used to compute the p-value of the test. We conclude that the two samples come from different distributions if the p-value is less than 0.05.

The entire procedure was coded in R language. The estimation of the Normal and Lognormal distributions was done using MASS package. The SuppDists library was used in the fit of the Johnson distributions. Finally, the two-sample KS test was done using STATS package.

For some of the data which could not be successfully fit using the above fitting techniques, cumulative probability graphs that result in an “S” type curve were produced to assist with interpretation of the data. This type of distribution has the advantage of providing an overall picture which shows the sum of deviation to any particular point [4].

Upon reviewing the statistically obtained data, it was decided that the median which is the middle value of the set of data is to be used as the average for the data analyzed as opposed to the mean value which is the arithmetic average, computed by adding up a collection of numbers and dividing by their count [4]. The median was chosen because it is not as sensitive to minimum and maximum values within the range of data analyzed. For data successfully fit with a distribution, the median and mean are equivalent. The minimum and maximum is represented by the range of data.

## 2.2 pH Profile as a Function of TSP Dissolution and Break Type

The pH profile was calculating using the rate of pool fill and the rate of TSP dissolution[5]. The TSP baskets are 2 feet tall with the bottom of the baskets positioned 6 inches above the floor. The baskets have TSP in them to a nominal depth 20 inches. For purposes of TSP submergence, the water volume calculation assumed the top of the TSP is at an elevation of 26 inches (2.17 feet). The containment building has a floor area of 12,300.9 ft<sup>2</sup> [1], thus, the pool reaches the top of the TSP when the pool volume is 26,642 ft<sup>3</sup>. Break flows for a MBLOCA have been estimated at 1200 lbm/s [6], which corresponds to a flow rate of 1150 ft<sup>3</sup>/min. The containment spray flow rate with two trains in operation is 5800 gpm (775 ft<sup>3</sup>/min) [1]. Thus, the total fill rate for the containment pool can be estimated at 1,925 ft<sup>3</sup>/min and the time to fill to a depth of 26 inches is 14 minutes. Since this time is relatively short and other uncertainties exist that affect the rate of TSP dissolution, the time to start TSP injection for the CHLE tests will be 15 minutes.

## 2.3 Acid Generation Due to Irradiation

The acid generation due to irradiation was previously calculated by STP using the Polestar QA software STARpH 1.05 code with the purposes of (1) determining the pH of the STP containment pool solution as a function of time following a LOCA using the alternative source term and (2) determining the maximum DF for the removal of elemental iodine form the containment atmosphere [7].

### 3 Design Input and Analyses

For each chemical constituent monitored by STP, the constituent concentration was reviewed. If the concentration of a chemical constituent was at trace levels (ppb or µg/L), it was eliminated from the list. If the concentration was significant (ppm or mg/L), the associated minimum, maximum and average concentrations based on the historical data was determined using one of the methods previously outlined.

#### 3.1 Containment Pool Volume

The containment pool solution is the sum of three possible sources of solution; the RCS, the RWST, and accumulators. Each source of solution injects into the pool as dictated by operational constraints resulting in a range of the final post-LOCA pool volume and mass. The range of pool solution mass used in the minimum and maximum pH calculation for STP [8] are referred to as design basis in this document, and are listed in Table 1. The average operational solution volumes and masses which were determined from statistical review of operating conditions and operational constraints [1] are listed in Table 2. The analysis of the operational solution mass for each source results in a “best estimate” which has a smaller final pool solution mass range (4.2-4.5 million lb) than the design basis range (3.7 – 5.4 million lb). The “best estimate” of the operation solution mass as listed in Table 2 was used in calculations of chemical constituents masses predicted to exist in the final pool volume.

Table 1: Design basis containment pool volume as a function of LOCA type [8].

Source	Min (lb)	Pool Contribution	Max (lb)	Pool Contribution
RWST	2,988,450	80%	4,505,980	84%
Accumulators	218,182	6%	228,015	4%
RCS	534,400	14%	631,700	12%
Total Mass	3,741,032	100%	5,365,695	100%

Table 2: “Best Estimate” Operating containment pool volume as a function of LOCA type [1].

Source	SBLOCA (lb)	Volume <sup>1</sup> (ft <sup>3</sup> )	Pool Contribution	MBLOCA and LBLOCA (lb)	Volume <sup>1</sup> (ft <sup>3</sup> )	Pool Contribution
RWST	3,630,265	58,238	86%	3,630,265	58,238	81%
Accumulators	0	0	0%	231,334	9,828	5%
RCS	612,644	3,711	14%	612,644	3,711	14%
Total Mass	4,242,909	68,066	100%	4,474,243	71,778	100%

<sup>1</sup> at 21 °C

### 3.2 Trisodium Phosphate

Trisodium phosphate dodecahydrate (TSP) is a buffer that exists in containment to maintain the pool pH greater or equal to pH 7 [9]. It is not present in any of the three sources of solution which contribute to the final pool volume. Instead, there are six baskets filled with a total of 11,500 to 15,100 lb of granular TSP [5] strategically located within the post-LOCA flood region of containment [9] which dissolves into solution in response to a LOCA. The range of TSP mass listed is a result of the density range associated with TSP ( $57 \pm 3 \text{ lb/ft}^3$ ) and loading procedures. Simply, the TSP in containment was not measured by weight, but calculated from volume. Each basket has two standardized marks that are two inches apart and is filled with granular TSP to any point between these marks [10]. A review of the basket levels [11] provides basis that the mass of TSP in containment is closer to the maximum cited range; therefore the TSP mass of 15,100 lb will be used as a scaling factor in the CHLE tests.

TSP dissolution has been calculated to occur within 80 minutes in the pool [9]. This was done using an experimentally obtained dissolution rate of  $0.7 \text{ lb/ft}^2$  which was determined from dissolution of a solid block of TSP in  $160^\circ\text{F}$  water with no agitation [12]. The total dissolution time is based on the assumptions that the baskets are completely submerged in approximately 15 minutes and that only the top and bottom surfaces of the basket are included in the surface area calculation; this allows for determination of an easily-calculated uniform rate of TSP dissolution. In an actual post-LOCA situation (LBLOCA and MBLOCA), all TSP surfaces would be exposed to the sump solution at initial temperatures exceeding  $200^\circ\text{F}$  with significant agitation and the baskets would be submerged within 15 minutes [8, 9] which suggest that the dissolution rate is conservative.

For SBLOCA, it may take longer than 15 minutes for the baskets to become submerged, the maximum initial temperature may be less than  $160^\circ\text{F}$ , agitation may not be as significant when compared to the larger LOCA scenarios and the final pool volume may be less than that of the larger LOCA scenarios. The mass of TSP in containment exposed the smaller final pool volume is not near the saturation limit for TSP; therefore the dissolution of TSP within solution may have a similar dissolution rate. The dissolution rate and the longer time required to fill the pool will result in a higher TSP concentration due to the volume dictated by the fill rate and possibly result in a characteristically different pH profile.

Since the review of STP records [11] indicate that the mass of TSP in the basket is reflective of the maximum range defined, the maximum mass (15,100 lb) and the median total pool volume ( $71,778 \text{ ft}^3$ ) for a LBLOCA/MBLOCA will be used to determine the TSP concentration ( $3.37 \text{ g/L}$ ) to be used in the CHLE tests. It has been determined that a SBLOCA will not be modeled in the CHLE tests, therefore this concentration was not calculated.

### 3.3 Boron

Boron in the form of boric acid is a neutron absorber that exists in the pool solution during any LOCA scenario. The three sources of solution (accumulators, RCS, and RWST) that contribute to the final pool volume as a result of a LOCA are maintained independently of each other possibly resulting in different

boron concentrations. The ranges of boron concentration for each source of solution used in the minimum and maximum pH design basis calculation are listed in Table 3 [5]. This range of boron concentrations with the range in solution volumes results in a wide range of boron mass within the containment pool.

Table 3: Design basis Boron concentration ranges for contributing sources.

Water Source	Minimum Concentration (mg/L)	Maximum Concentration (mg/L)
Accumulators	2700	3000
RWST	2800	3000
RCS	0	3500

Review of historical data showed that the sources of solution that contribute to the final pool volume as a result of a LOCA are maintained within a narrower band of concentrations (Table 4) as compared to the design basis. The last seven years of historical accumulator data was processed to provide a thorough analysis, since they are monitored less frequently. Since the RCS and RWST are monitored frequently, only the last two years of historical data was processed. The following sections explain the review of this data.

Table 4: Operating Boron concentration ranges for contributing sources.

Water Source	Minimum Concentration (mg/L)	Maximum Concentration (mg/L)
Accumulators	2767	2952
RWST	2895	2962
RCS	3.7	3105

### 3.3.1 RCS Boron

#### 3.3.1.1 RCS Boron Analyses

The historical review of operation data for boron concentration observed in the RCS sources of both units is presented by Figure 1. A histogram for each RCS (Figures 2 and 4) was created for the statistical analysis to identify a minimum, maximum, and average boron concentration. As shown by Figure 2 and 4, the boron concentration as a function of time does not fit a normal Gaussian distribution; the concentration is not random but instead is controlled to vary the power output of the reactor. Thus, relative cumulative frequency graphs (Figures 3 and 5) were prepared to examine the distribution of the data. On the basis of these graphs, the median was determined to be a suitable value to use in the 30-day CHLE tests.

Title: Determination of the initial pool chemistry for the CHLE test

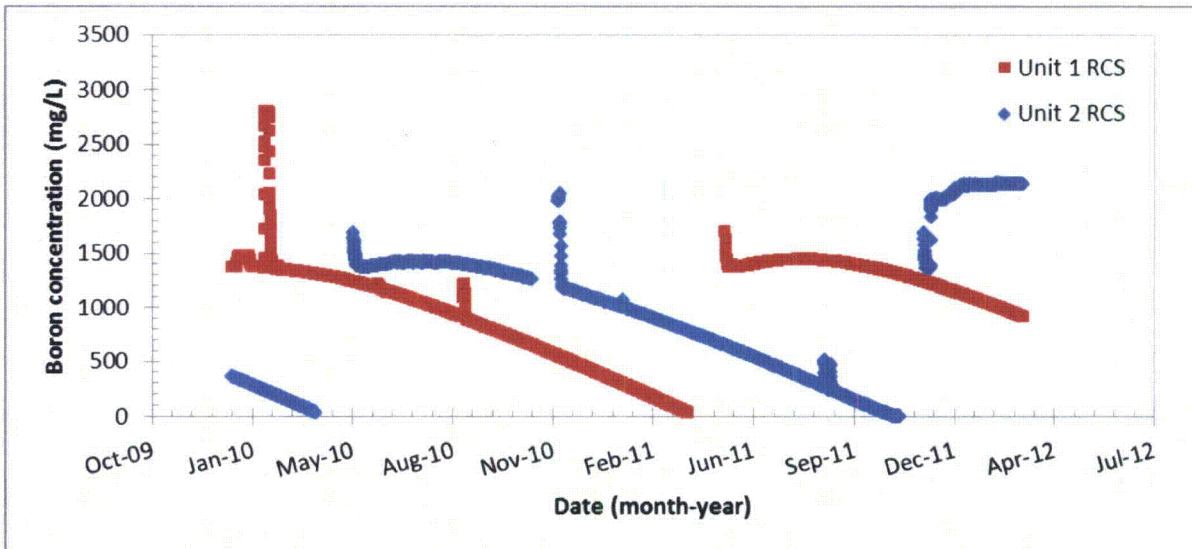


Figure 1: Boron concentration for Unit 1 and 2 RCS as a function of time.

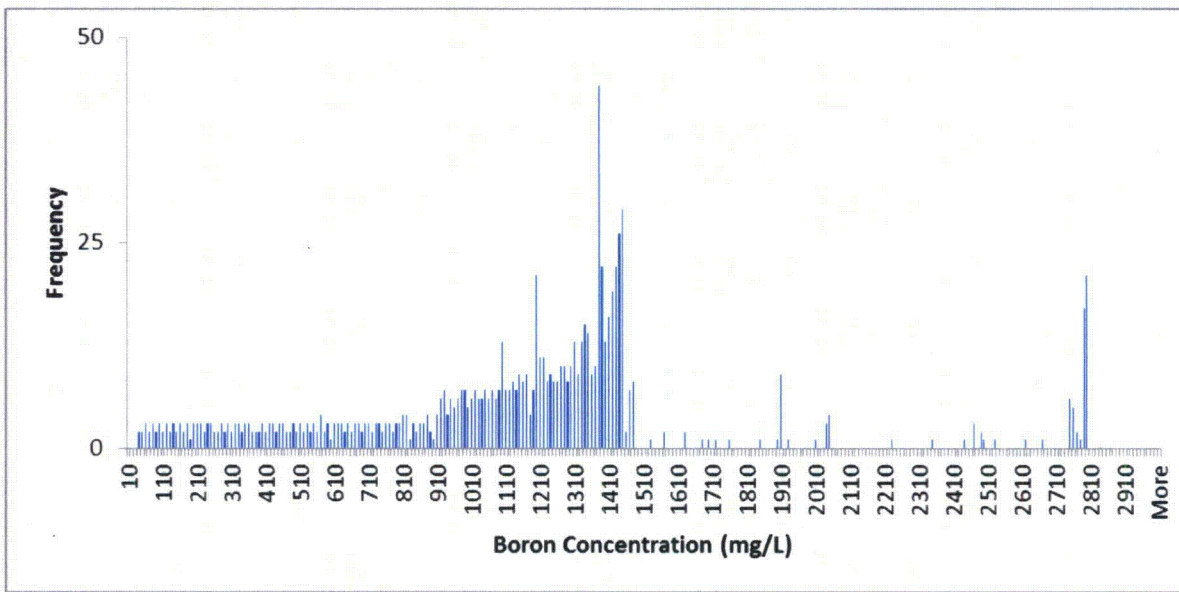


Figure 2: RCS 1 Boron histogram.

Table 5: Statistical RCS 1 data (Figure 2).

RCS 1	
Mean (mg/L)	1185
Standard Error (mg/L)	19
Median (mg/L)	1218
Mode (mg/L)	1374
Standard Deviation (mg/L)	584
Kurtosis	2
Skewness	1
Minimum (mg/L)	35
Maximum (mg/L)	2797
Count	915

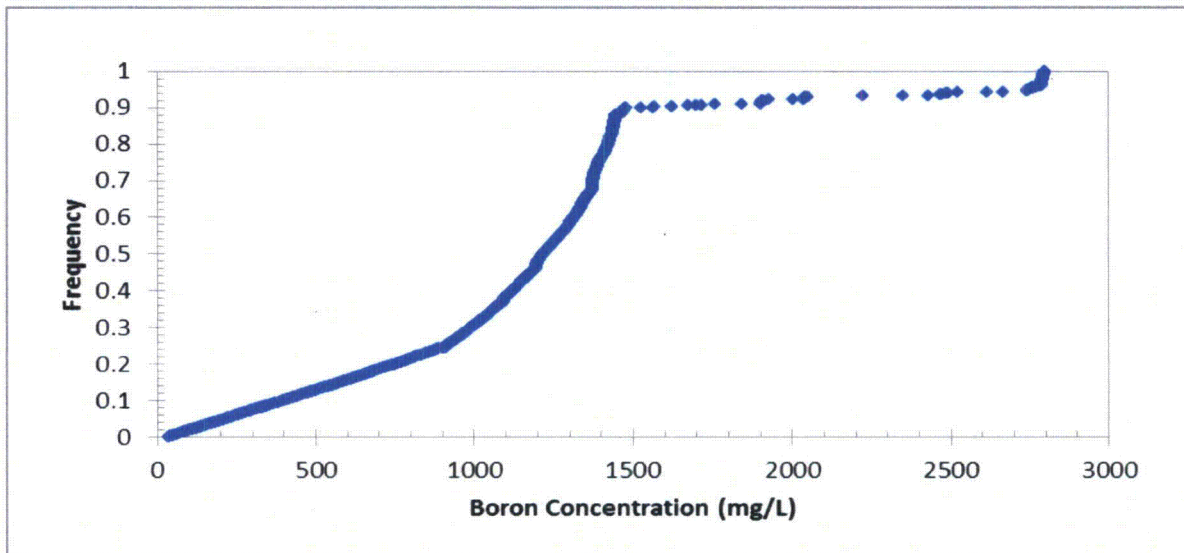


Figure 3: RCS 1 Boron relative cumulative frequency graph.

Title: Determination of the initial pool chemistry for the CHLE test

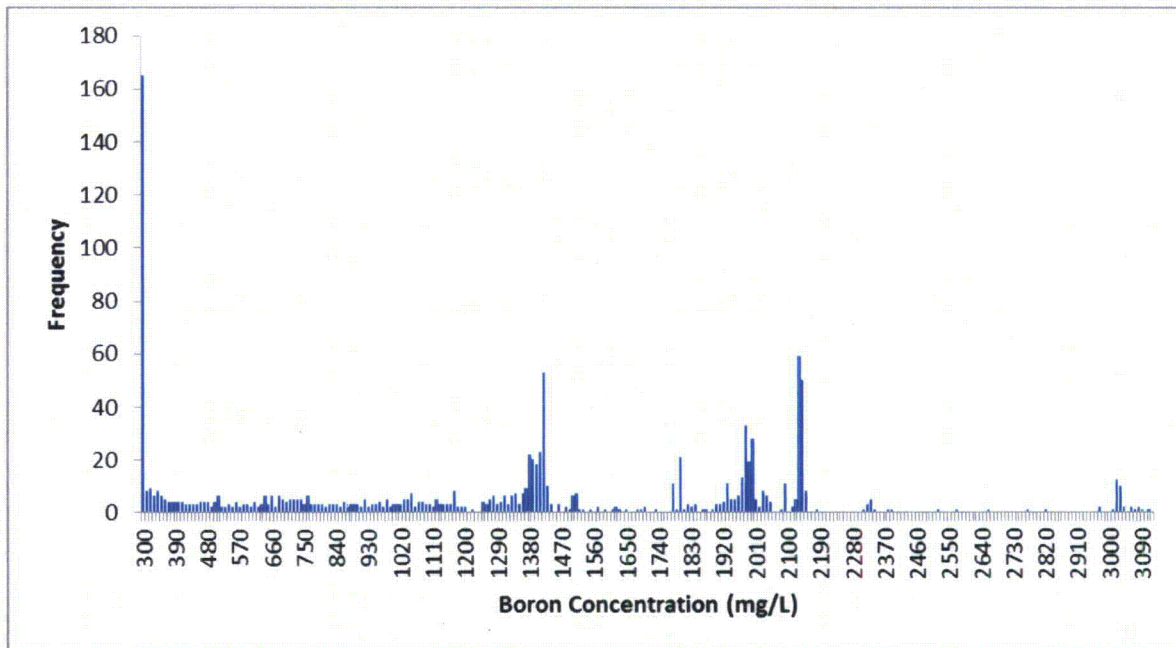


Figure 4: RCS 2 Boron histogram.

Table 6: Statistical RCS 2 data (Figure 4).

<i>RCS 2 B</i>	
Mean (mg/L)	1265.6
Standard Error (mg/L)	22.5
Median (mg/L)	1372.0
Mode (mg/L)	1416.0
Standard Deviation (mg/L)	760.3
Kurtosis	-0.8
Skewness	0.1
Minimum (mg/L)	3.7
Maximum (mg/L)	3105.0
Count	1138.0

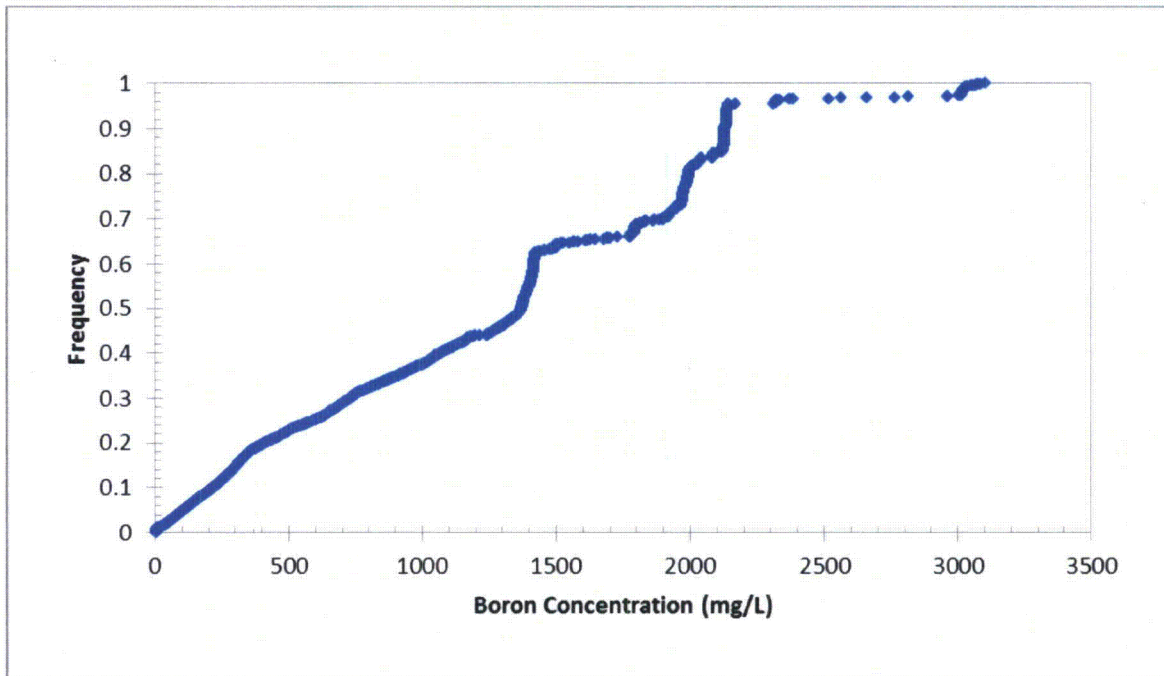


Figure 5: RCS 2 Boron relative cumulative frequency graph.

### 3.3.1.2 RCS Boron Concentration Results

Summary of results from the RCS boron analysis is presented in Table 7. The median value will be used as the average value for the RCS boron concentration. It should also be noted that the difference in pH using the range of boron concentrations (minimum, maximum, and median values) for the RCS in combination with the median boron concentrations determined for the RWST and accumulator with the TSP concentration determined for the 30 Day test, only resulted in a pH ranging between 7.09 and 7.24. This is within experimental accuracy of  $\pm 0.2$  pH units.

Table 7: Summary of Boron concentrations.

Source	Minimum (mg/L)	Maximum (mg/L)	Median (mg/L)
RCS 1	35	2797	1218
RCS 2	3.7	3105	1372

### 3.3.2 RWST Boron Concentration

#### 3.3.2.1 RWST Boron Concentration Analyses

The historical data (Figure 6) was successfully statistically fit (Figures 7 and 8) resulting in a statistically valid median (Tables 8 and 9) for both sets of data reflective of the RWST of units 1 and 2.



Title: Determination of the initial pool chemistry for the CHLE test

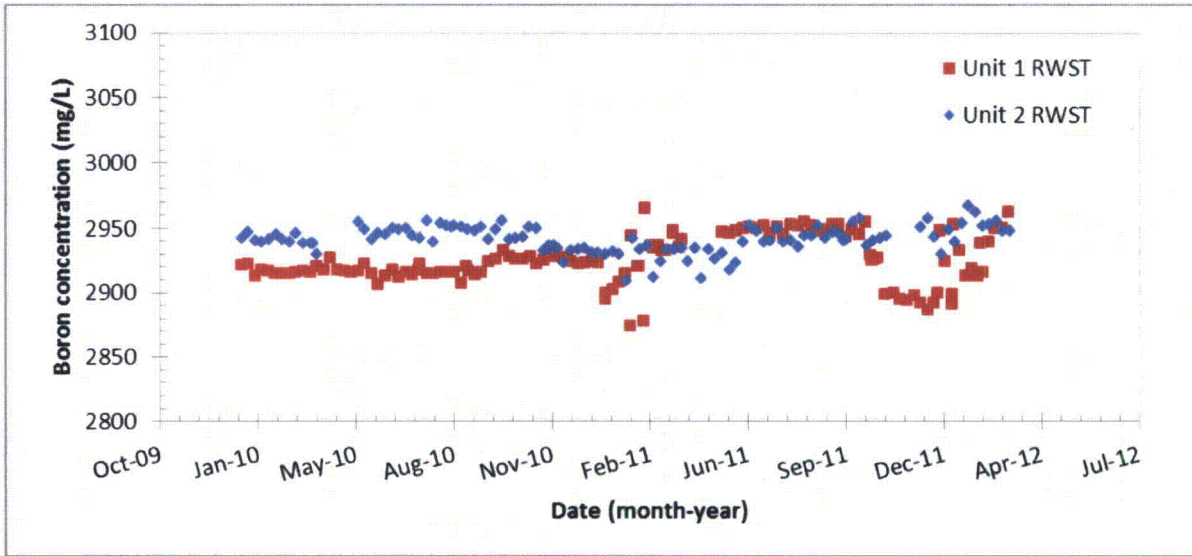


Figure 6: Boron concentration in Unit 1 and Unit 2 RWST as a function of time.

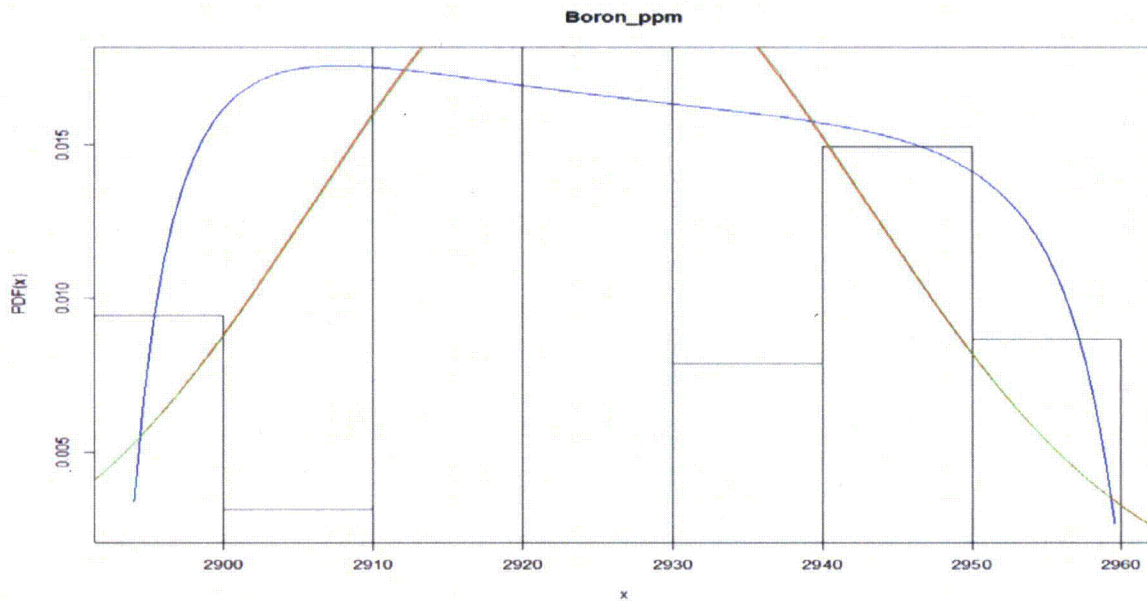


Figure 7: Probability distribution function of RWST 1 Boron concentration. The blue line is the Johnson fit and the green line is the normal fit.

Table 8: Probability distribution statistics for RWST 1 Boron concentrations.

Parameters	Normal	Lognormal	Johnson
Min (mg/L)	2895		
Max (mg/L)	2958		
Mean (mg/L)	2925	2925	2920
Median (mg/L)	2925	2925	2925
Variance (mg/L) <sup>2</sup>	328	328	344

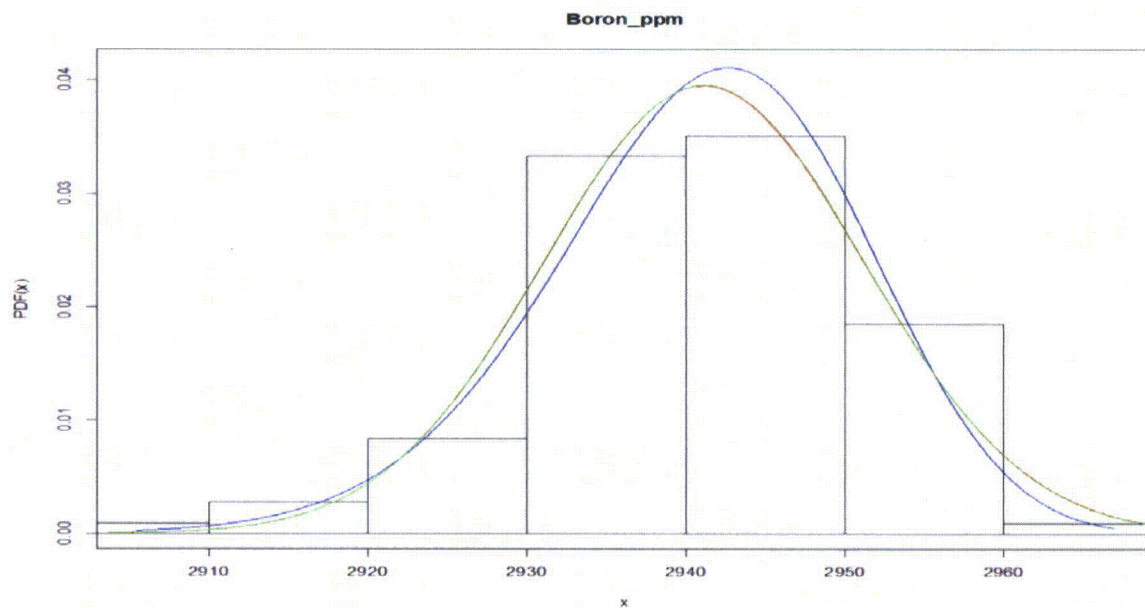


Figure 8: Probability distribution function of RWST 2 Boron concentration. The blue line is the Johnson fit and the green line is the normal fit.

Table 9: Probability distribution statistics for RWST 2 Boron concentrations.

Parameters	Normal	Lognormal	Johnson
Min (mg/L)	2916		
Max (mg/L)	2962		
Mean (mg/L)	2941 <sup>1</sup>	N/A	N/A
Median (mg/L)	2941 <sup>1</sup>	N/A	N/A
Variance (mg/L) <sup>2</sup>	108 <sup>1</sup>	N/A	N/A

<sup>1</sup> The raw data associated with Figure 8 was not available at the time of report. The associated information was calculated using excel.

### 3.3.2.2 RWST Boron Concentration Results

Both RWST sources fit a Gaussian distribution using the different fitting procedures. Since all the fits result in a very similar median, the normal distribution fit median is the median to be used. A summary of boron concentrations observed in the RWST sources of both units, Table 10.

Table 10: Statistical results from the Boron concentration analyses of the RWST.

Source	Minimum (mg/L)	Maximum (mg/L)	Median (mg/L)
RWST 1	2895	2958	2925
RWST 2	2916	2962	2941

### 3.3.3 Accumulator Boron Concentration

#### 3.3.3.1 Accumulator Boron Concentration Analyses

Historical data (Figure 9) for accumulator 1A could not be fit resulting in a normal Gaussian distribution (Figure 10) because the declining concentration from February 2008 to April 2012 did not follow a random pattern. Thus, a relative cumulative frequency graph (Figure 11) was prepared to examine the distribution of the data. On the basis of the relative cumulative frequency, the median was determined to be a suitable value to use in the 30-day CHLE tests. Parameters from the statistical analysis are shown in Table 11. All other accumulators were successfully fit with a normal, log normal, and Johnson distributions (Figures 12-16) resulting in mean and median values that were nearly identical for the various distributions (Tables 12-16).

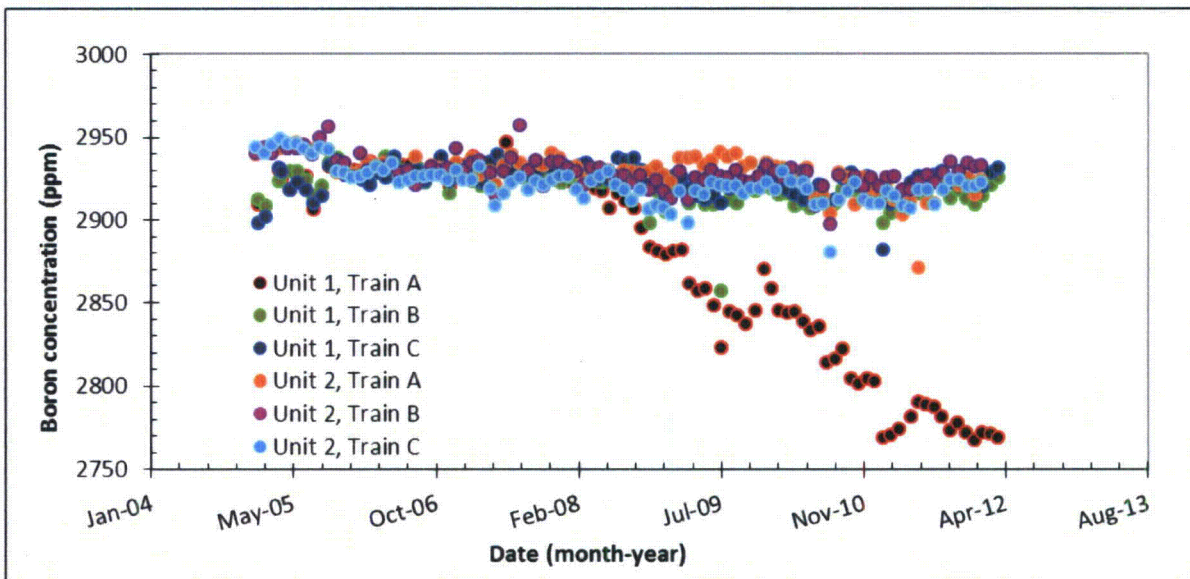


Figure 9: Boron concentration of Accumulators as a function of time.

Title: Determination of the initial pool chemistry for the CHLE test

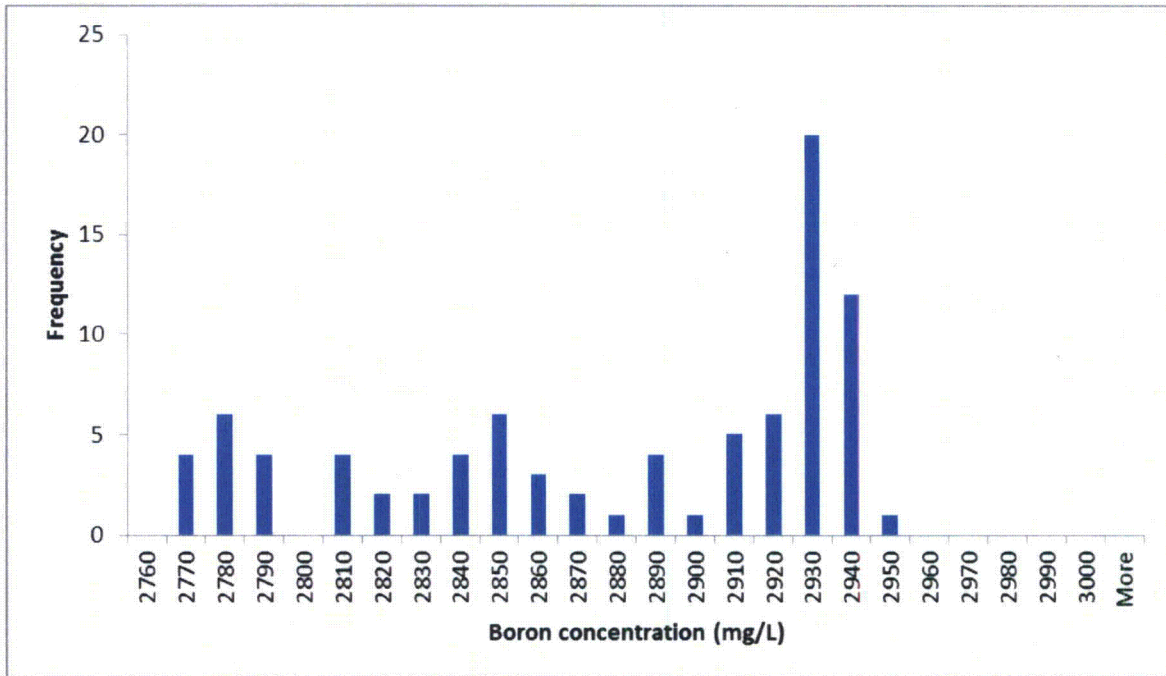


Figure 10: Accumulator 1A Boron histogram.

Table 11: Statistics for Accumulator 1A (Figure 10).

ACC 1A	
Mean (mg/L)	2874.4
Standard Error (mg/L)	6.3
Median (mg/L)	2906.0
Mode (mg/L)	2927.0
Standard Deviation (mg/L)	59.0
Kurtosis	3485.2
Skewness	-1.2
Minimum (mg/L)	-0.6
Maximum (mg/L)	2767.0
Count	2947.0
Mean (mg/L)	87.0

Title: Determination of the initial pool chemistry for the CHLE test

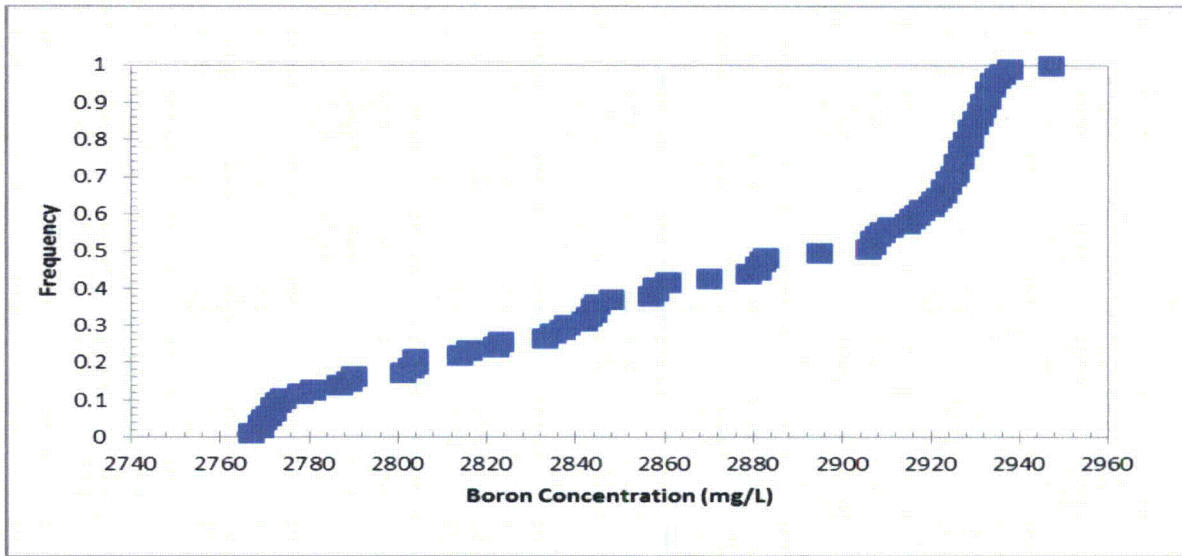


Figure 11: Accumulator 1A Boron relative cumulative frequency graph.

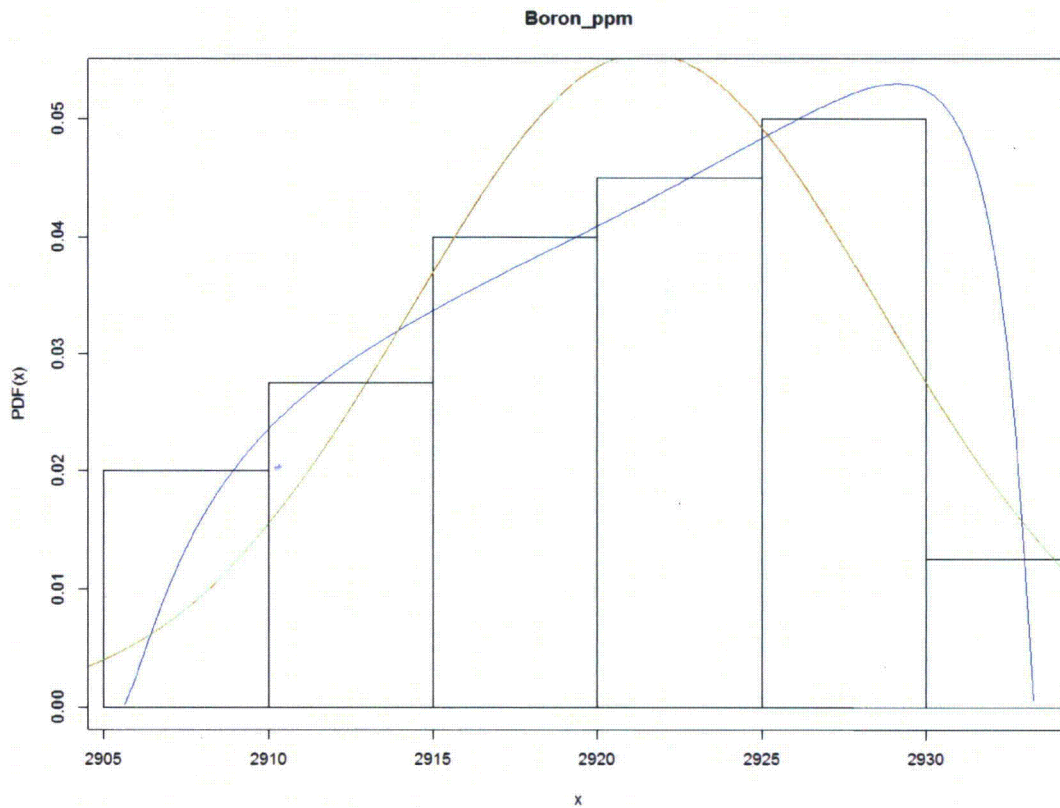


Figure 12: Probability distribution function of Accumulator 1B Boron concentration. The blue line is the Johnson fit and the green line is the normal fit.

Table 12: Probability distribution function for Accumulator 1B Boron concentrations.

Parameters	Normal	Lognormal	Johnson
Min (mg/L)	2906		
Max (mg/L)	2933		
Mean (mg/L)	2922	2922	2916
Median (mg/L)	2922	2922	2923
Variance (mg/L) <sup>2</sup>	52	52	81

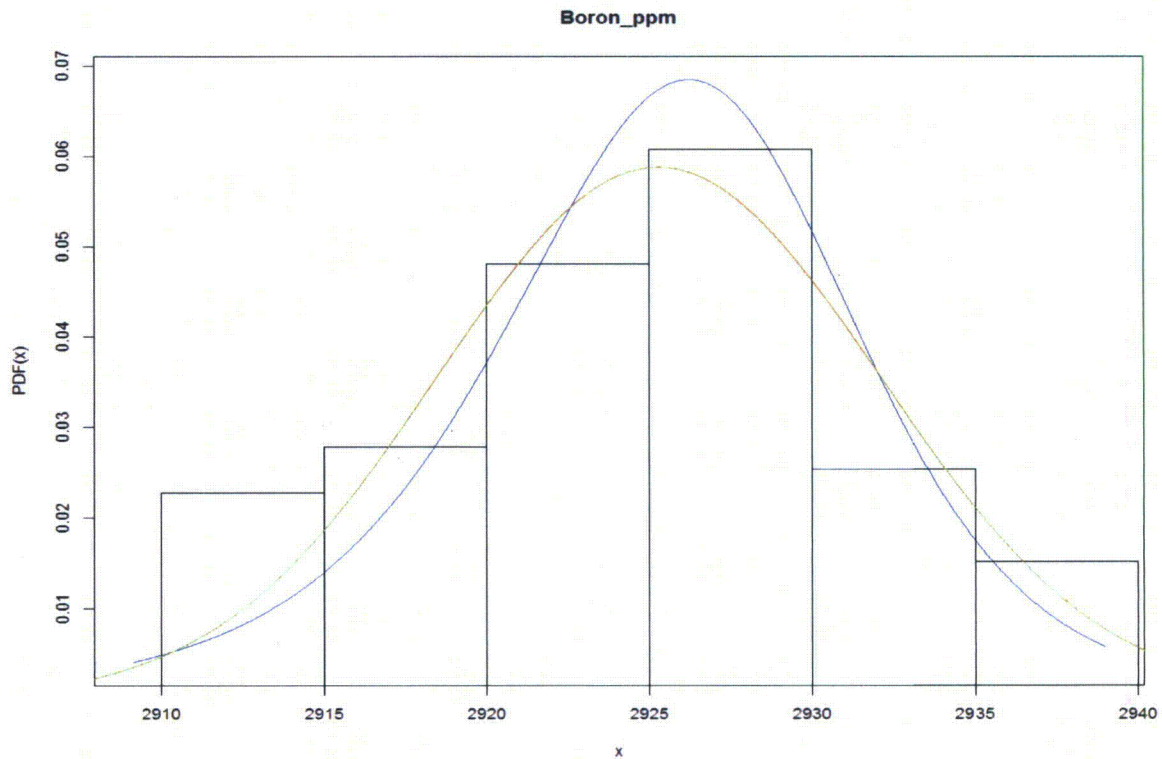


Figure 13: Probability distribution function of Accumulator 1C Boron concentration. The blue line is the Johnson fit and the green line is the normal fit.

Table 13: Probability distribution function for Accumulator 1C Boron concentrations.

Parameters	Normal	Lognormal	Johnson
Min (mg/L)	2906		
Max (mg/L)	2942		
Mean (mg/L)	2925	2925	2925
Median (mg/L)	2925	2925	2926
Variance (mg/L) <sup>2</sup>	46	46	48

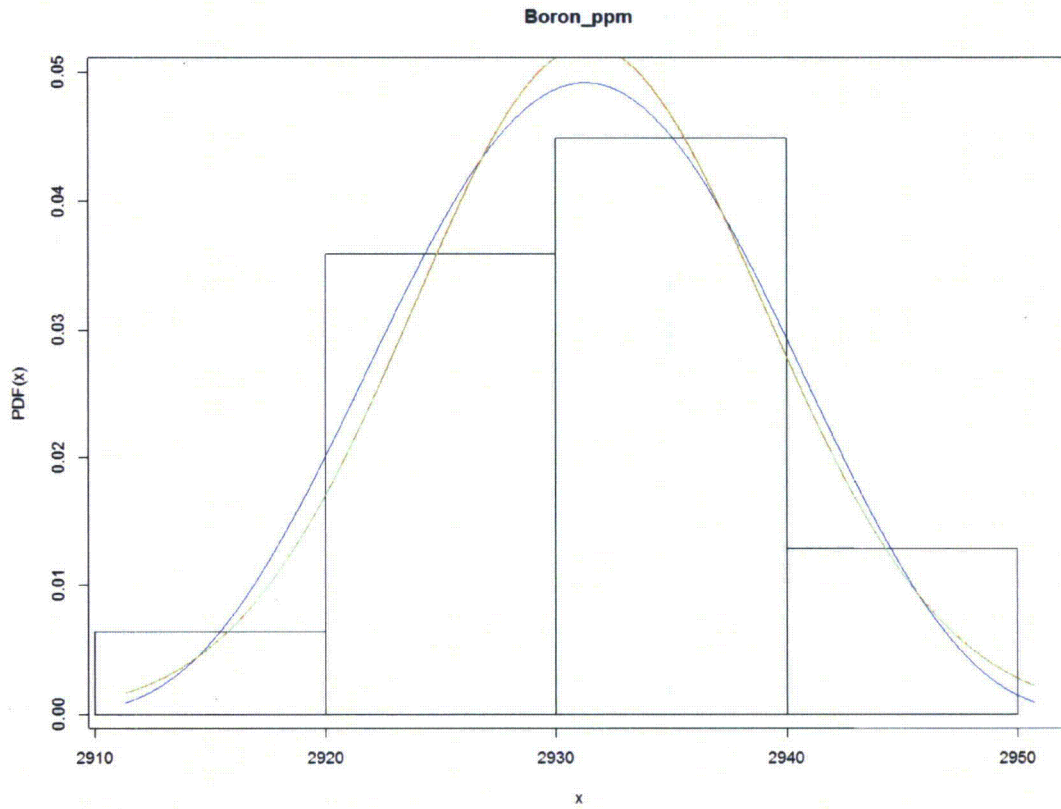


Figure 14: Probability distribution function of Accumulator 2A Boron concentration. The blue line is the Johnson fit and the green line is the normal fit.

Table 14: Probability distribution statistics for Accumulator 2A Boron concentrations.

Parameters	Normal	Lognormal	Johnson
Min (mg/L)	2914		
Max (mg/L)	2951		
Mean (mg/L)	2931	2931	2925
Median (mg/L)	2931	2931	2931
Variance (mg/L) <sup>2</sup>	59	59	90

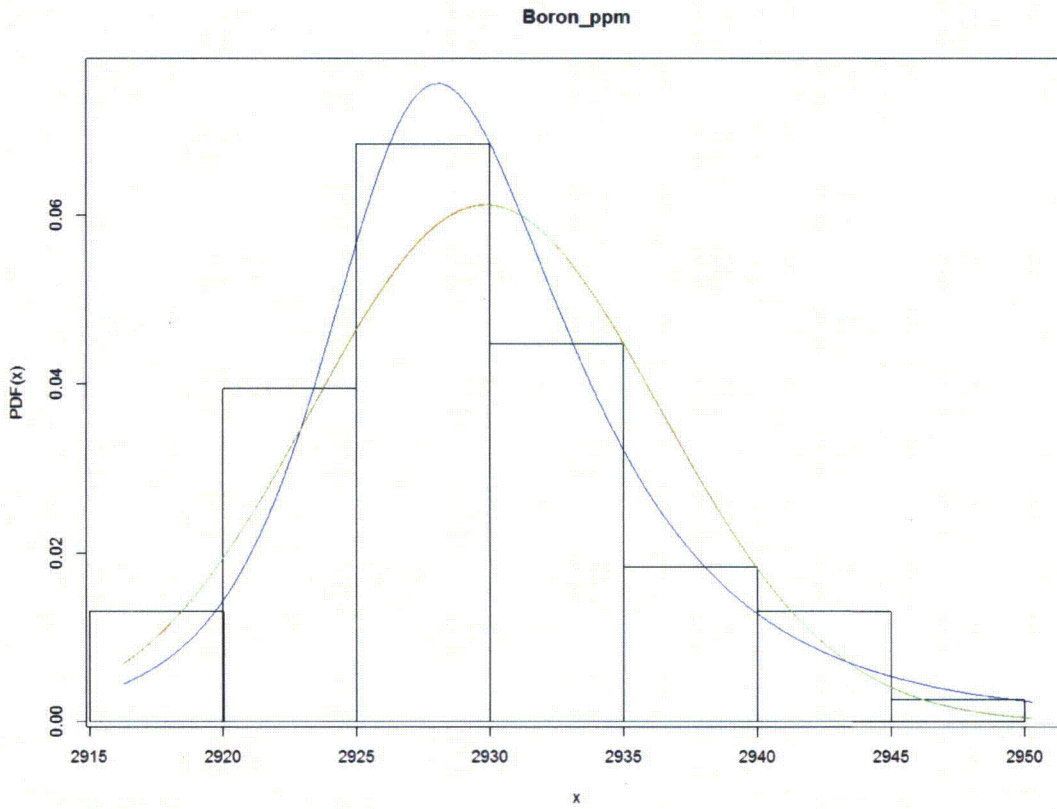


Figure 15: Probability distribution function of Accumulator 2B Boron concentration. The blue line is the Johnson fit and the green line is the normal fit.

Table 15: Probability distribution statistics for Accumulator 2B Boron concentrations.

Parameters	Normal	Lognormal	Johnson
Min (mg/L)	2917		
Max (mg/L)	2950		
Mean (mg/L)	2930	2930	2930
Median (mg/L)	2930	2930	2929
Variance (mg/L) <sup>2</sup>	43	42	59



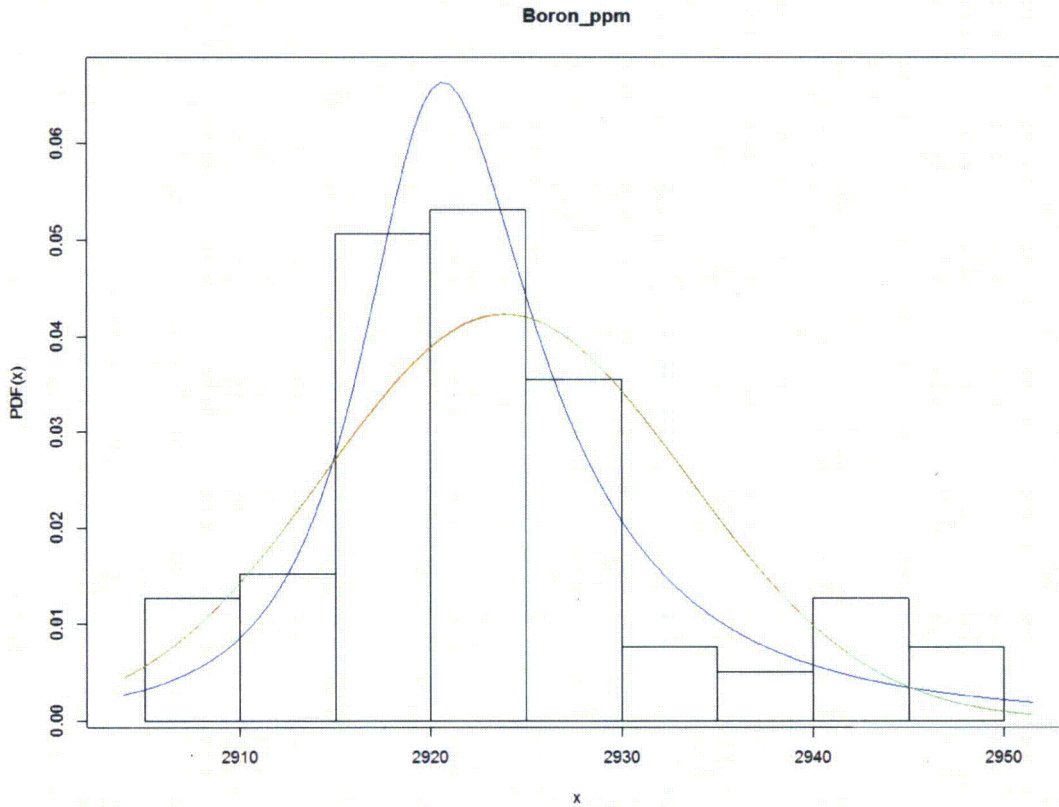


Figure 16: Probability distribution function of Accumulator 2C Boron concentration. The blue line is the Johnson fit and the green line is the normal fit.

Table 16: Probability distribution statistics for Accumulator 2C Boron concentrations.

Parameters	Normal	Lognormal	Johnson
Min (mg/L)	2904		
Max (mg/L)	2952		
Mean (mg/L)	2924	2924	2924
Median (mg/L)	2924	2924	2922
Variance (mg/L) <sup>2</sup>	89	89	184

### 3.3.3.2 Accumulator Boron Concentration Results

All accumulators except accumulator 1A were fit well with a normal distribution; thus, the median determined from the normal distribution will be used as the accumulator boron concentration in the 30-day CHLE tests. For accumulator 1A, the median from the raw data will be used in the 30-day CHLE tests. The accumulator boron concentrations used in the CHLE tests are summarized in Table 17.

Table 17: Summary of accumulator concentration ranges.

Source	Median (mg/L)	Minimum (mg/L)	Maximum (mg/L)
Accum 1A	2906	2767	2947
Accum 1B	2922	2906	2933
Accum 1C	2925	2906	2942
Accum 2A	2931	2914	2951
Accum 2B	2930	2917	2950
Accum 2C	2924	2904	2952

### 3.3.4 Final Boron Concentration Results

The 30 Day CHLE test will use the average of the values resulting from the complete analysis values listed in Table 18 for boron concentrations. The values listed in Table 19 will be covered within the bounds of the lab test.

Table 18: Boron concentration used to determine the concentration in the 30-day CHLE tests.

Source	Unit 1 (mg/L)	Unit 2 (mg/L)
	Median	Median
RCS	1218	1372
Accum A	2906	2931
Accum B	2922	2930
Accum C	2925	2924
RWST	2925	2941

Table 19: Boron concentrations to be investigated in the CHLE tests.

Source	Unit 1 (mg/L)		Unit 2 (mg/L)	
	Minimum	Maximum	Minimum	Maximum
RCS	35	2797	3.7	3105
Accum A	2767	2947	2914	2951
Accum B	2906	2933	2917	2950
Accum C	2906	2942	2904	2952
RWST	2895	2958	2916	2962

### 3.4 Silicon

The SFP contains Boraflex panels that contain significant amounts of silicon in the form of silicon dioxide (silica). As the panels degrade over time, silica is released to the SFP resulting in a long term increasing trend for SFP silica concentration. During refueling outages, the refueling cavity is flooded from the RWST and hydraulic contact between the SFP and reactor cavity is established to facilitate fuel movement between the reactor and SFP. The hydraulic contact and fuel movement allows silica to migrate to the reactor cavity and increase the silica concentration of the cavity water.

Following core reload, the reactor cavity is drained back to the RWST resulting in increased RWST silica concentrations compared to pre-outage levels. The RWST is not used as a RCS makeup source during normal power operations. RCS dilution and makeup is performed using the Reactor Makeup Water Storage Tank (RMWST) which contains demineralized water along with the Boric Acid Tanks (BATS) which provide a source of borated water for blended makeup.

The silica concentration in the RWST is managed by the use of a Boric Acid Recovery System (BARS) which is used periodically to lower silica concentration in the RWST. The BARS is efficient in removing silica although most of the boron is retained in solution. The only approved method to lower SFP silica is by small drain and refill evolutions. The RWST and/or SFP cleanup evolutions are performed as needed to prevent silica concentration from impacting the RCS chemistry. The RCS is maintained at < 1 ppm silica at 100% power, while the silica concentration in the RWST and accumulators can be higher. Therefore the concentration of the pool solution will be dependent on the concentration of silica and associated solution volume of each contributing source to the final pool volume.

### 3.4.1 RCS Silicon Concentration

#### 3.4.1.1 RCS Silicon Analyses

The historical review of operation data for silicon concentration as silica dioxide observed in the RCS sources of both units is presented by Figure 17. A histogram for each RCS (Figures 18 and 19) was created to begin the statistical analysis to identify a minimum, maximum and average silicon concentration as silica dioxide (Table 20 and 21). The data did not fit a normal Gaussian distribution for either unit.

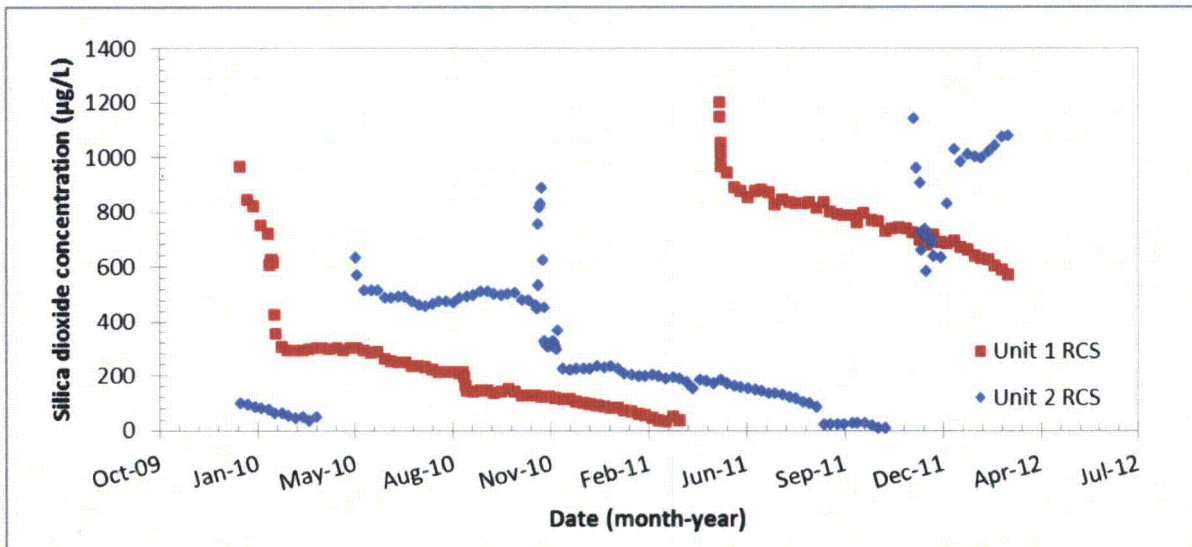


Figure 17: Silicon as silica dioxide concentration in Unit 1 and Unit 2 RCS as a function of time.

Title: Determination of the initial pool chemistry for the CHLE test

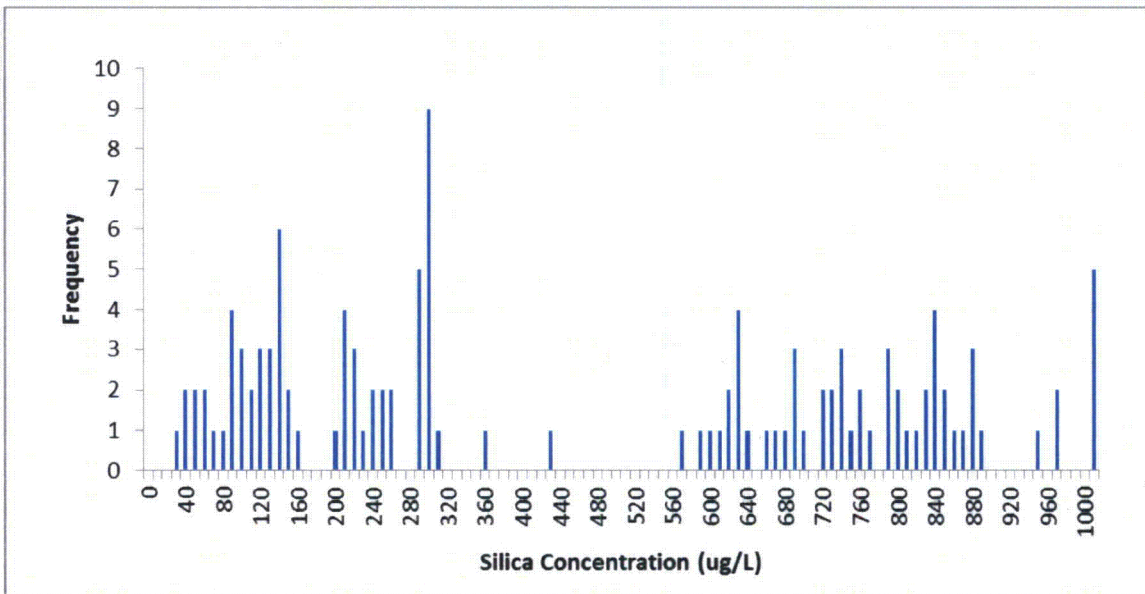


Figure 18: RCS 1 Silica histogram.

Table 20: Statistics for RCS 1 Silica (Figure 18).

<i>RCS 1 Silica</i>	
Mean (µg/L)	352.7
Standard Error (µg/L)	34.2
Median (µg/L)	234.0
Mode (µg/L)	962.0
Standard Deviation (µg/L)	318.7
Kurtosis	0.1
Skewness	1.2
Minimum (µg/L)	30.0
Maximum (µg/L)	1196.0
Count	87.0

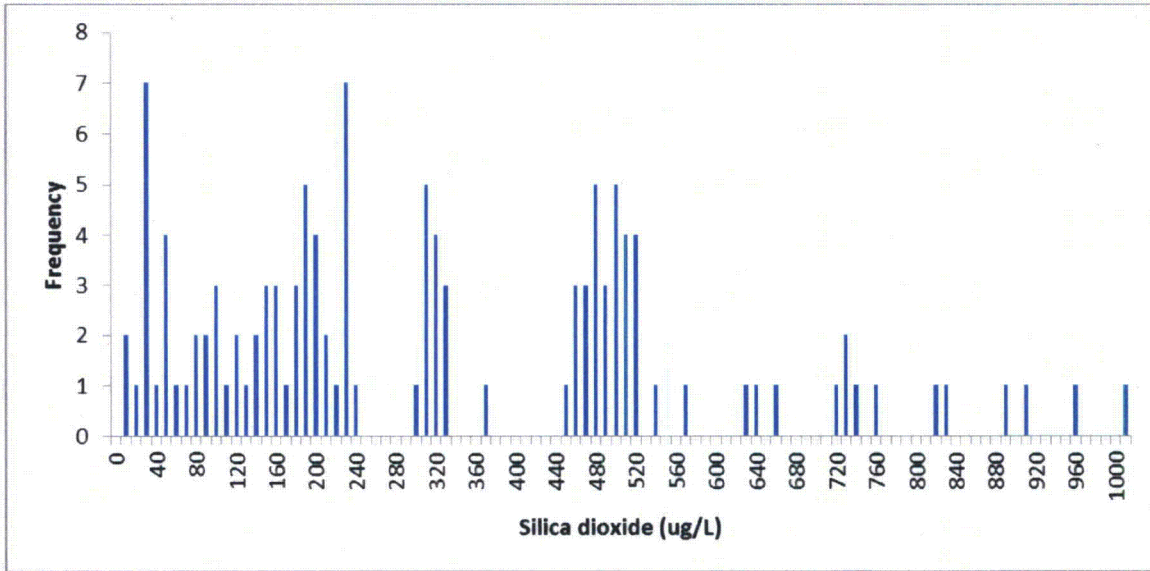


Figure 19: RCS 2 Silica histogram.

Table 21: Statistics for RCS 2 Silica (Figure 19).

<i>RCS 2 Silica</i>	
Mean ( $\mu\text{g/L}$ )	320.9
Standard Error ( $\mu\text{g/L}$ )	22.3
Median ( $\mu\text{g/L}$ )	230.5
Mode ( $\mu\text{g/L}$ )	317.0
Standard Deviation ( $\mu\text{g/L}$ )	242.0
Kurtosis	58544.4
Skewness	0.4
Minimum ( $\mu\text{g/L}$ )	0.9
Maximum ( $\mu\text{g/L}$ )	5.0
Count	1140.0
Mean ( $\mu\text{g/L}$ )	118.0

### 3.4.1.2 RCS Silicon results

Since silicon is known to passivate aluminum [15], it was determined silicon will not be added in the tank test. The maximum and minimum concentrations (Table 20 and 21) observed at STP will be captured in the bench tests.

## 3.4.2 RWST Silicon Concentration

### 3.4.2.1 RWST Silicon Analyses

The historical review of operation data for silicon concentration as silica dioxide observed in the RCS sources of both units is presented by Figure 20. A histogram for each RCS (Figures 21 and 22) was created to begin the statistical analysis to identify a minimum, maximum and average silicon

Title: Determination of the initial pool chemistry for the CHLE test

concentration as silica dioxide (Table 22 and 23). The data did not fit a normal Gaussian distribution for either unit.

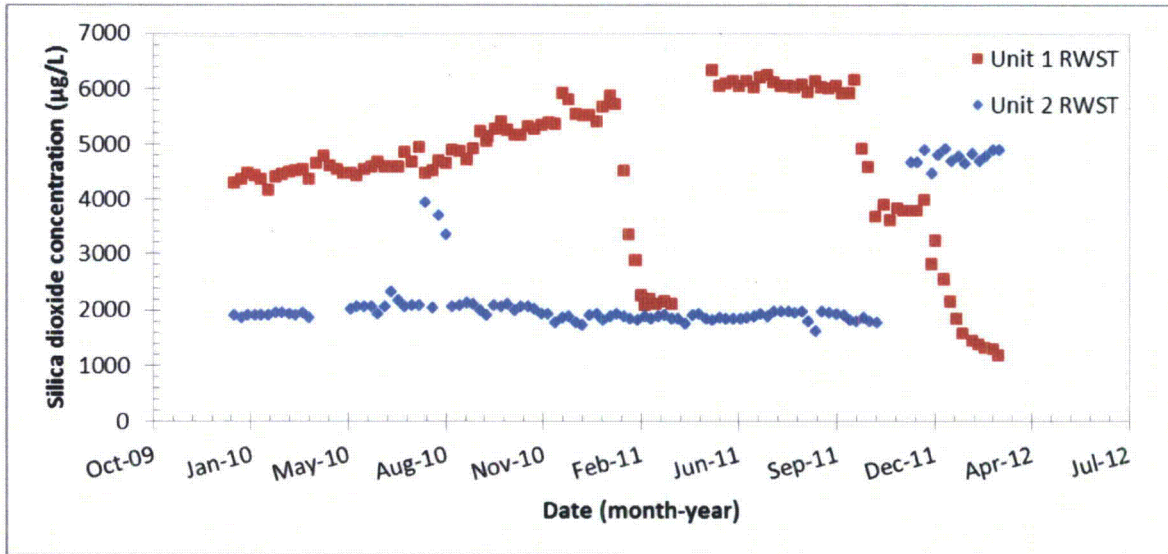


Figure 20: Silicon as silica dioxide concentration in Units 1 and 2 RWST as a function of time.

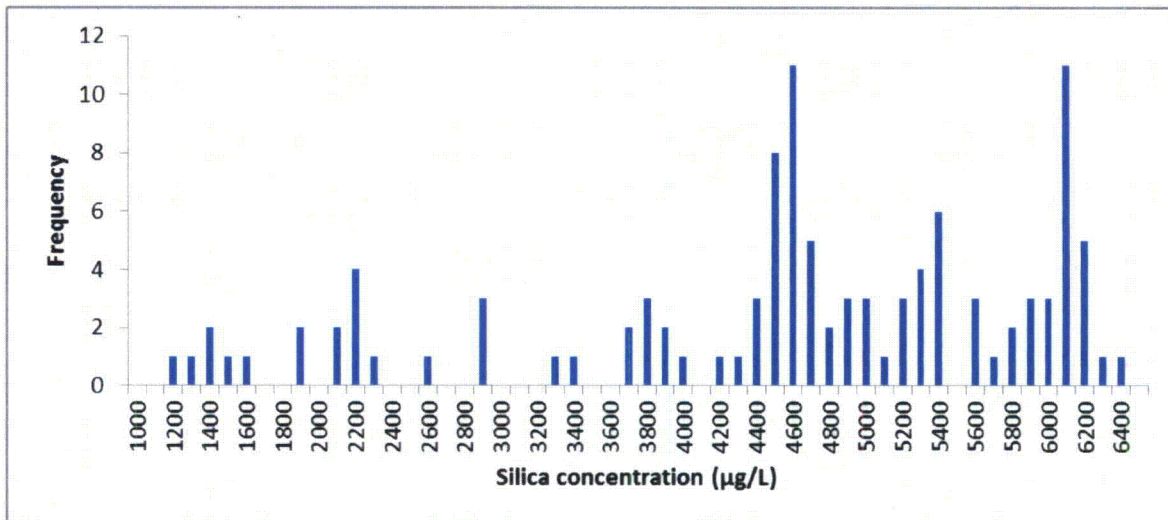


Figure 21: RWST 1 Silica histogram.

Table 22: Statistics for RWST 1 Silica (Figure 21).

<i>RWST 1 Silica</i>	
Mean ( $\mu\text{g/L}$ )	4518.8
Standard Error ( $\mu\text{g/L}$ )	131.4
Median ( $\mu\text{g/L}$ )	4665.0
Mode ( $\mu\text{g/L}$ )	4470.0
Standard Deviation ( $\mu\text{g/L}$ )	1378.6
Kurtosis	-0.1
Skewness	-0.9
Minimum ( $\mu\text{g/L}$ )	1175.0
Maximum ( $\mu\text{g/L}$ )	6330.0
Count	110.0

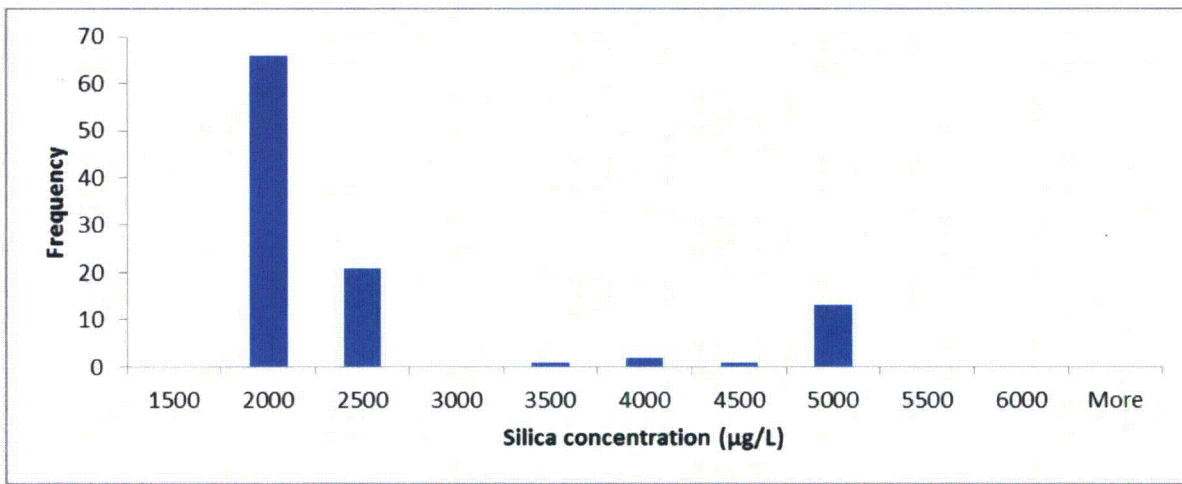


Figure 22: RWST 2 silica histogram.

Table 23: Statistics for RWST 2 (Figure 22).

<i>RWST 2 Silica</i>	
Mean ( $\mu\text{g/L}$ )	2358.0
Standard Error ( $\mu\text{g/L}$ )	98.3
Median ( $\mu\text{g/L}$ )	1930.0
Mode ( $\mu\text{g/L}$ )	2060.0
Standard Deviation ( $\mu\text{g/L}$ )	1002.6
Kurtosis	1.9
Skewness	1.9
Minimum ( $\mu\text{g/L}$ )	1620.0
Maximum ( $\mu\text{g/L}$ )	4910.0
Count	104.0

### 3.4.2.2 RWST Silicon Results

Again, since silicon is known to passivate aluminum, it was determined that silicon will not be added in the tank tests. The maximum and minimum concentrations observed at STP (Table 22 and 23) will be captured in the bench tests.

### 3.4.3 Silicon Results

Since silicon can passivate aluminum and lower the corrosion rate, it was decided not to add silicon in the tank test. The minimum and maximum concentration of silicon as silica dioxide for the analysis of historical data, Table 24, will be covered in the bench scale test.

Table 24: Results associated with Silica histogram.

Unit	Minimum Concentration (µg/L)	Maximum Concentration (µg/L)
RCS 1	30	1196
RCS 2	0.9	1140
RWST 1	1175	6330
RWST 2	1620	4910

## 3.5 Lithium

Lithium in the form of lithium hydroxide is present only in the RCS and is used to maintain the RCS solution pH = 7.2 at 592 °F. The concentration of lithium hydroxide is variable in the RCS solution and is determined by the concentration of boric acid in solution. The concentration of lithium in the pool solution will be less than in the RCS and will depend on the associated solution volume of each contributing source to the final pool volume.

### 3.5.1 RCS Lithium Concentration

#### 3.5.1.1 Lithium RCS Analyses

The historical trend of the lithium concentration observed in the RCS for both Unit 1 and 2, Figure 23, was not processed statistically because the lithium concentration is determined by the boron concentration which has already been determined for the CHLE tests.



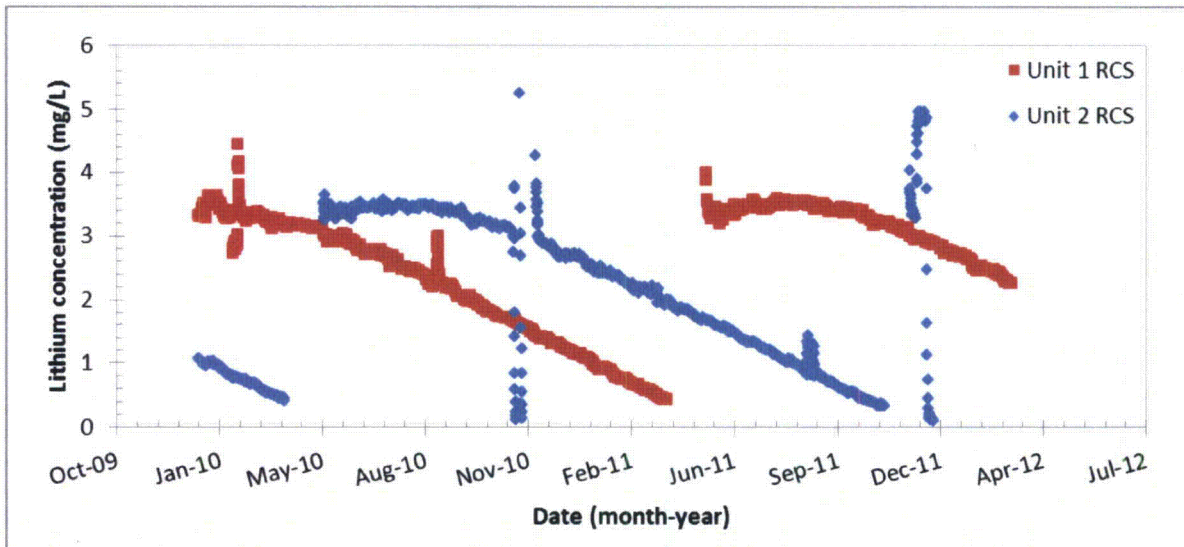


Figure 23: Lithium concentration in Unit 1 and Unit 2 RCS as a function of time.

### 3.5.1.2 Lithium RCS Results

While historical plant data was obtained for the lithium concentration, the lithium concentration is dictated by the boron concentration to maintain pH in the RCS. Therefore, the median boron concentration dictates lithium concentration and the only lithium contribution to the pool is from the RCS.

Table 25: LBLOCA and MBLOCA concentration of Boron and Lithium in RCS.

Unit	Median Boron Concentration (mg/L)	Lithium Concentration in RCS (mg/L)
RCS 1	1218	2.9
RCS 2	1372	3.3

## 3.6 Zinc

Zinc in the form of zinc acetate is added to the RCS as a dose rate mitigation control. The concentration of zinc varies between 5 to 10 ppb and depends on the time elapsed over the course of the fuel cycle. The concentration of zinc in of the pool solution will be less than that found in the RCS and will depend on the associated solution volume of each contributing source to the final pool volume.

### 3.6.1 RCS Zinc Concentration

#### 3.6.1.1 RCS Zinc Analyses

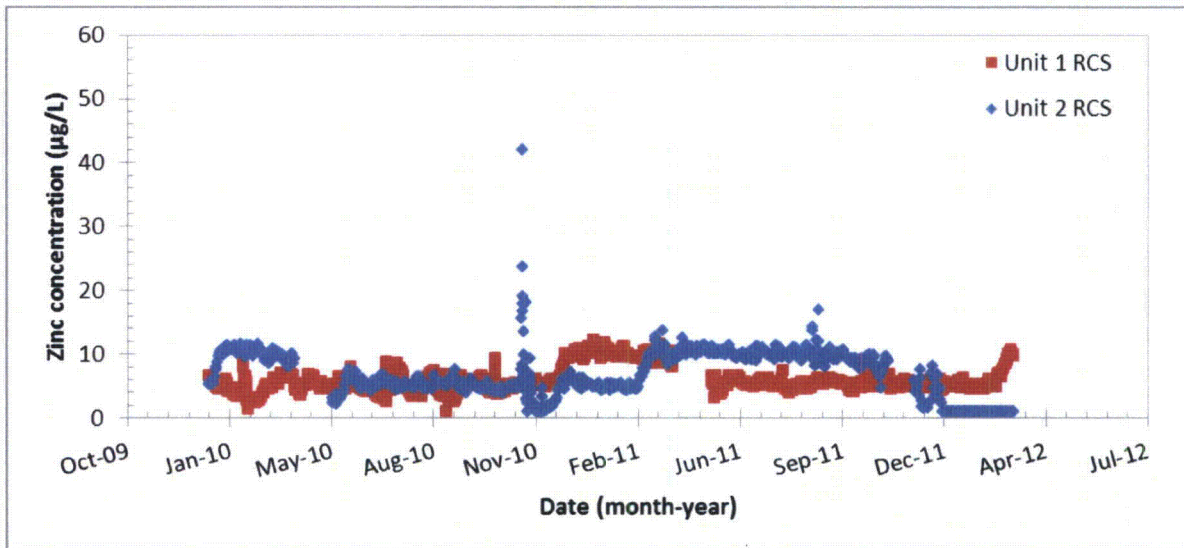


Figure 24: Zinc concentration in Unit 1 and 2 RCS as a function of time.

### 3.6.1.2 RCS Zinc Results

Zinc acetate is added only to the RCS, which is only approximately 15% of total pool volume. It is below 10 ppb at any given time. Therefore, the contribution of zinc from chemicals added at STP will not be included in the CHLE analyses.

## 3.7 Environmental Contribution (O<sub>2</sub> and CO<sub>2</sub>)

Oxygen and carbonate in the form of carbon dioxide is present in containment because of its presence in the atmosphere.

### 3.7.1 Oxygen

#### 3.7.1.1 Oxygen Analysis

While there may be trace amount of oxygen in the RWST or the accumulators (not monitored for), there is very little to no oxygen in the RCS (Figure 29). During a LOCA event, the atmosphere is the largest source of oxygen in containment which is in equilibrium with the pool solution. During outages, the air in containment exchanges with the ambient atmosphere, which contains 21 percent oxygen by volume. The containment building at STP contains 3,374,000 ft<sup>3</sup> of air[13]. Thus, the total quantity of oxygen in the air in the containment building prior to a LOCA is 57,900 lb.

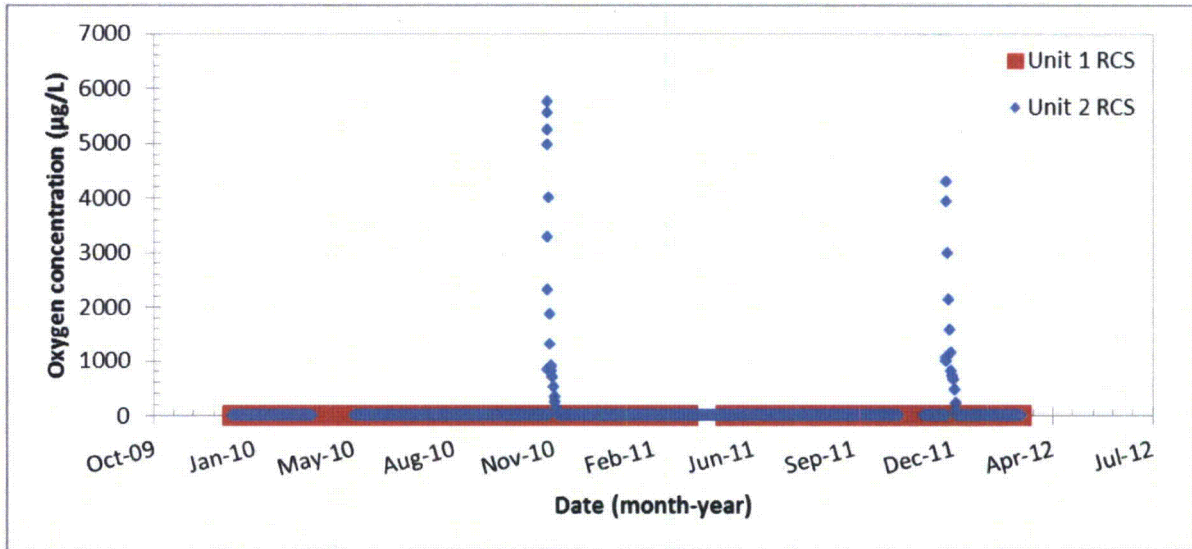


Figure 25: Oxygen concentration in Unit 1 and Unit 2 RCS as a function of time.

During a LOCA, water spills from RCS piping or is sprayed from the containment spray system and thus has opportunity for oxygen to transfer from the air to the water. Oxygen has relatively low solubility in water; the saturation concentration is 8.12 ppm at 25 °C. Oxygen partitions between the gas and liquid phases according to Henry's Law, which is dependent on temperature. Assuming that no oxygen is initially present in the RCS, RWST, or accumulator water, there is sufficient oxygen in the air to essentially reach the saturation concentration. The equilibrium concentration in the pool water as a function of temperature is shown in Figure 16. The total quantity of oxygen in the pool water at equilibrium will be 12.3 lb at 85 °C to 30.4 lb at 25 °C. Since this is less than 0.06 percent of the oxygen inside containment, the pool solution will not be limited with respect to oxygen.

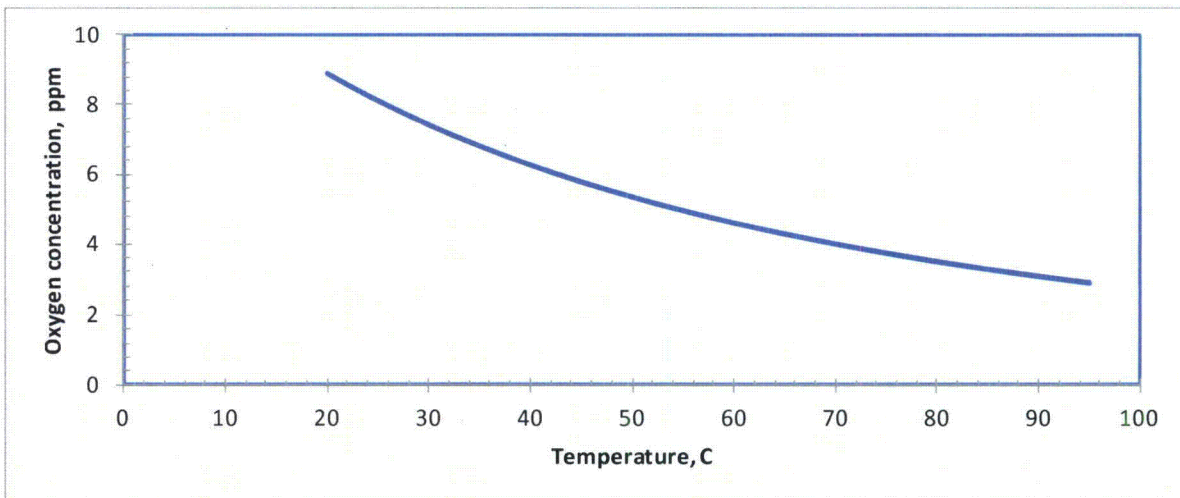


Figure 26: Decrease in oxygen concentration as a function of temperature.

### 3.7.1.2 Oxygen Results

The CHLE experiments will be conducted with oxygen present. The solution will initially be oxygenated when the tank is filled, the solution will be exposed to the atmosphere inside the tank, and the lid will occasionally be opened, so no special provisions are necessary to provide oxygen to the system.

## 3.7.2 Carbonate

### 3.7.2.1 Carbonate Analysis

A potential chemical interaction in a LOCA is reaction between calcium (from leaching of concrete or other materials) and carbonate to form calcium carbonate precipitate. Carbonate can enter the pool solution as carbon dioxide from the air. During a LOCA, water spills from RCS piping or is sprayed from the containment spray system and thus has opportunity for carbon dioxide to transfer from the air to the water. Carbon dioxide has relatively low solubility in water; the saturation concentration is 0.55 ppm at 25 °C. Carbon dioxide partitions between the gas and liquid phases according to Henry's Law, which is dependent on temperature. Furthermore, once carbon dioxide is present in the water, it transforms to bicarbonate and carbonate, with the relative concentration of each species being dependent on pH.

During outages, the air in containment exchanges with the ambient atmosphere, which contains 390 ppm carbon dioxide by volume. The containment building at STP contains 3,374,000 ft<sup>3</sup> of air [13]. Thus, the total quantity of carbon dioxide in the air in the containment building prior to a LOCA is 148 lb. Assuming that no carbonate is initially present in the RCS, RWST, or accumulator water, there is sufficient carbon dioxide in the air to essentially reach the saturation concentration at low pH. At higher pH, the fraction of carbon dioxide that transitions to carbonate increases and at high pH the total carbonate present in the containment pool during a LOCA would be lower than the total carbonate present in a completely open system. At pH 7.2 the total carbonate present in the containment pool at STP would be about 90 percent of the carbonate present in a completely open system. Thus, allowing the CHLE tank to be open to the atmosphere provides a slightly conservative (slightly higher) concentration of carbonate compared to the STP containment during a LOCA.

### 3.7.2.2 Carbonate Results

The CHLE experiments will be conducted with carbon dioxide present. The solution will initially be aerated when the tank is filled, the solution will be exposed to the atmosphere inside the tank, and the lid will occasionally be opened, so no special provisions are necessary to provide carbon dioxide to the system.

## 3.7.3 Summary of Environmental Contribution results

No special provisions are necessary to control the interaction between the atmosphere and pool solution in the CHLE tests.

### 3.8 Impurities

Magnesium, aluminum, calcium, copper, and sulfate are impurities that are monitored because they may influence disposition of scale on the fuel rods. Corrosion products such as fluoride, chloride and nickel are another form of impurities which are monitored to access corrosion concern. These impurities, if present in significant concentrations, may influence the overall pool chemistry of the CHLE analysis. Therefore the historical trends were reviewed to determine inclusion and concentration to be used in the analysis.

#### 3.8.1 Impurities

##### 3.8.1.1 Impurity Analyses

Historical trends of impurity data for the RWST and RCS are listed below. There is no surveillance data for these impurities for the accumulators; thus the accumulators are not included in this analysis.

##### RCS Related Graphs

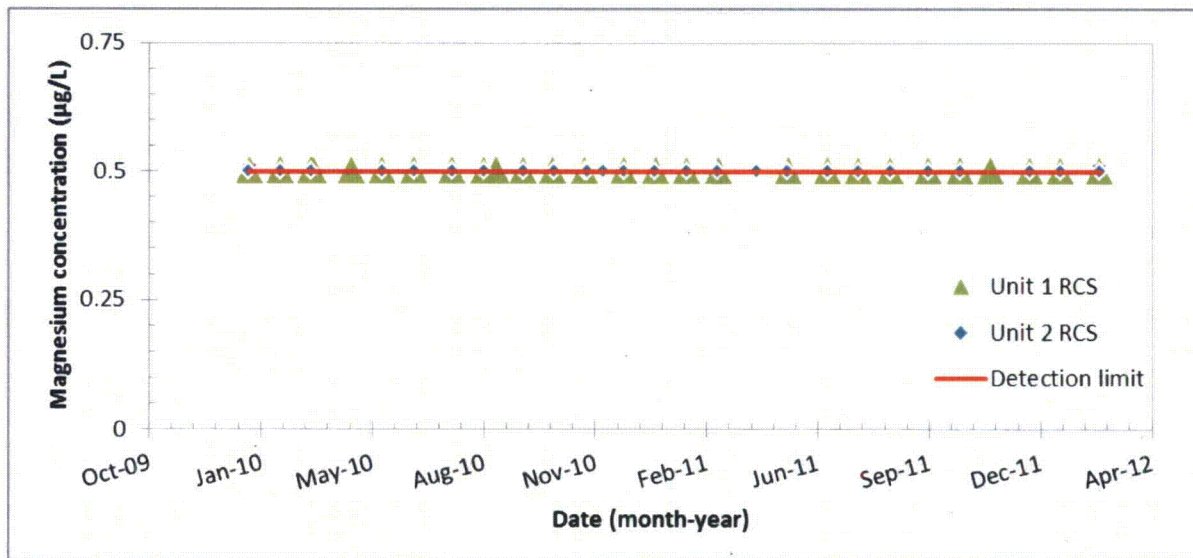


Figure 27: Magnesium concentration in Unit 1 and Unit 2 RCS as a function of time.

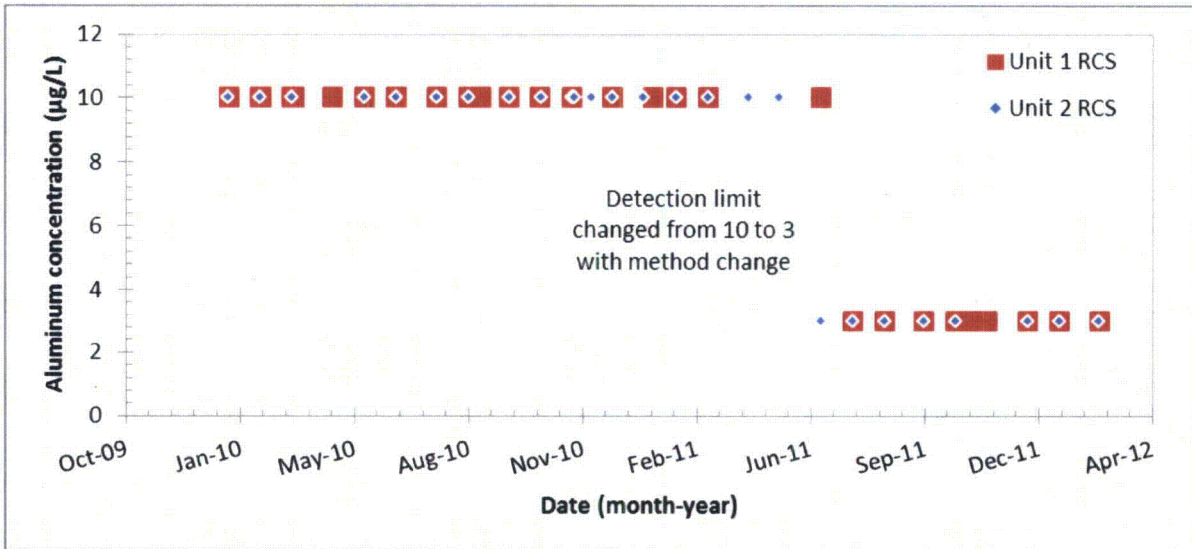


Figure 28: Aluminum concentration in Unit 1 and Unit 2 RCS as a function of time.

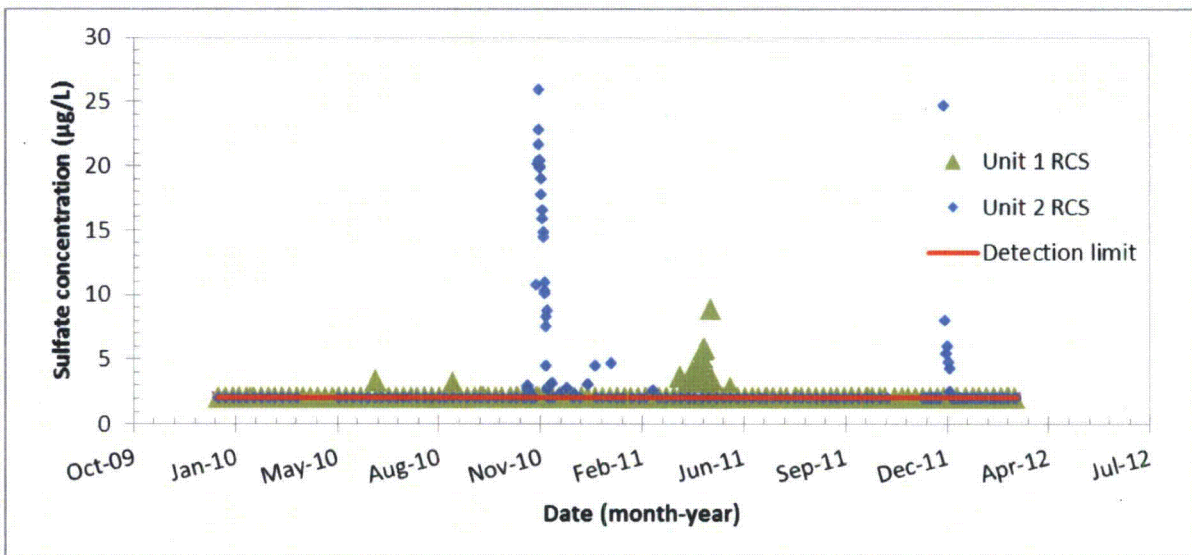


Figure 29: Sulfate concentration in Unit 1 and Unit 2 RCS as a function of time.

Title: Determination of the initial pool chemistry for the CHLE test

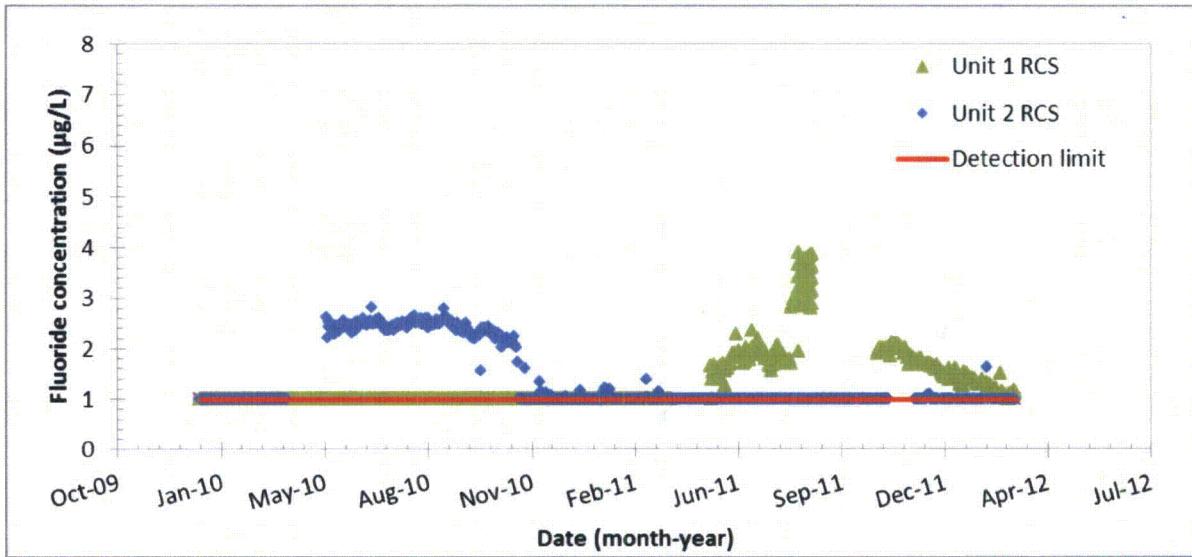


Figure 30: Fluoride concentration in Unit 1 and Unit 2 RCS as a function of time.

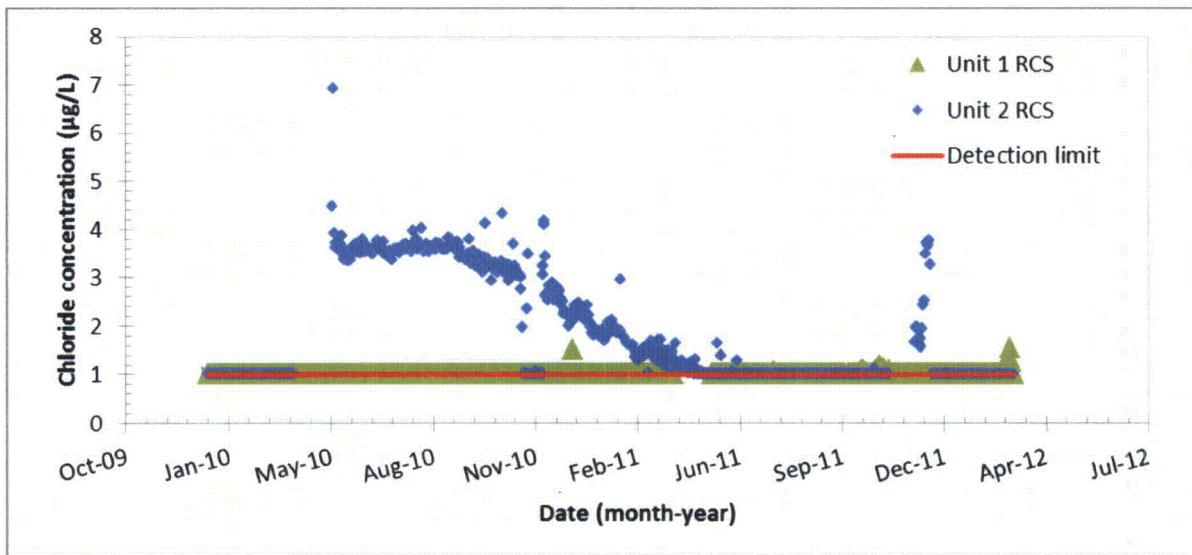


Figure 31: Chloride concentration in Unit 1 and Unit 2 RCS as a function of time.

Title: Determination of the initial pool chemistry for the CHLE test

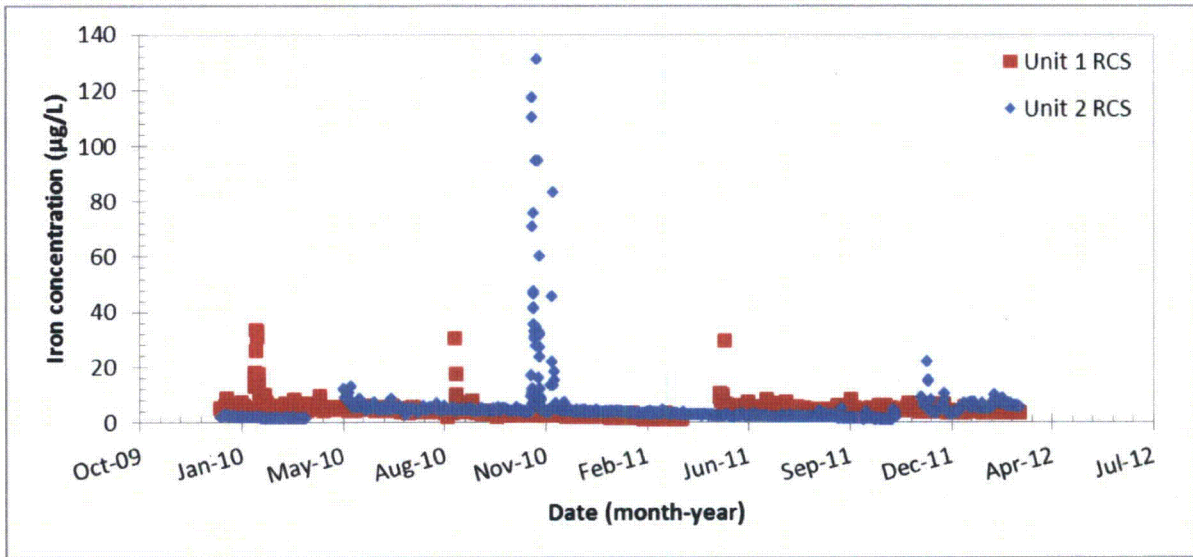


Figure 32: Iron concentration in Unit 1 and Unit 2 RCS as a function of time.

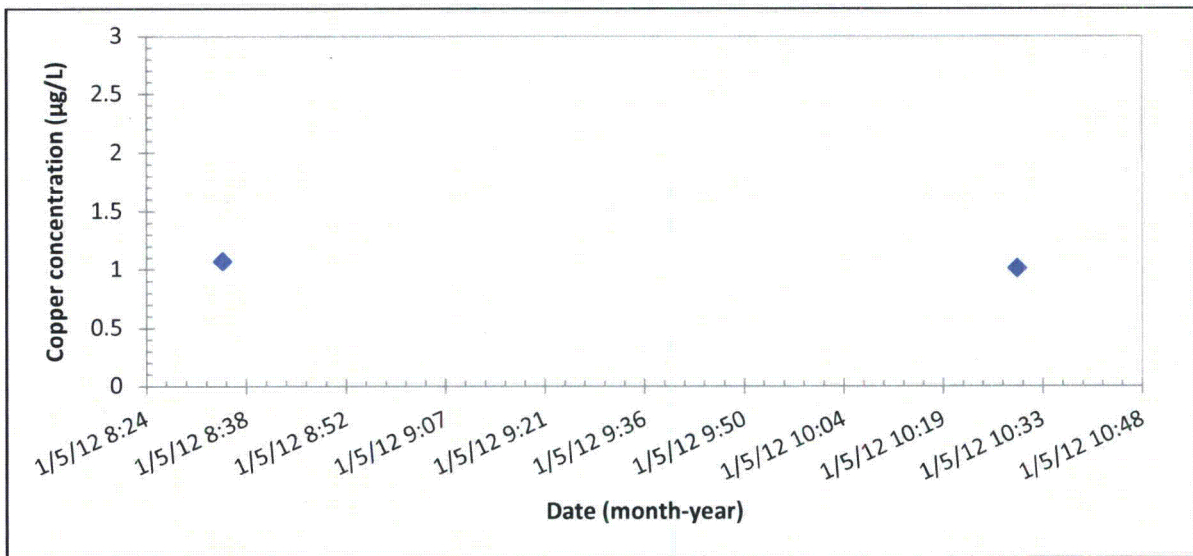


Figure 33: Copper concentration in Unit 1 RCS as a function of time.



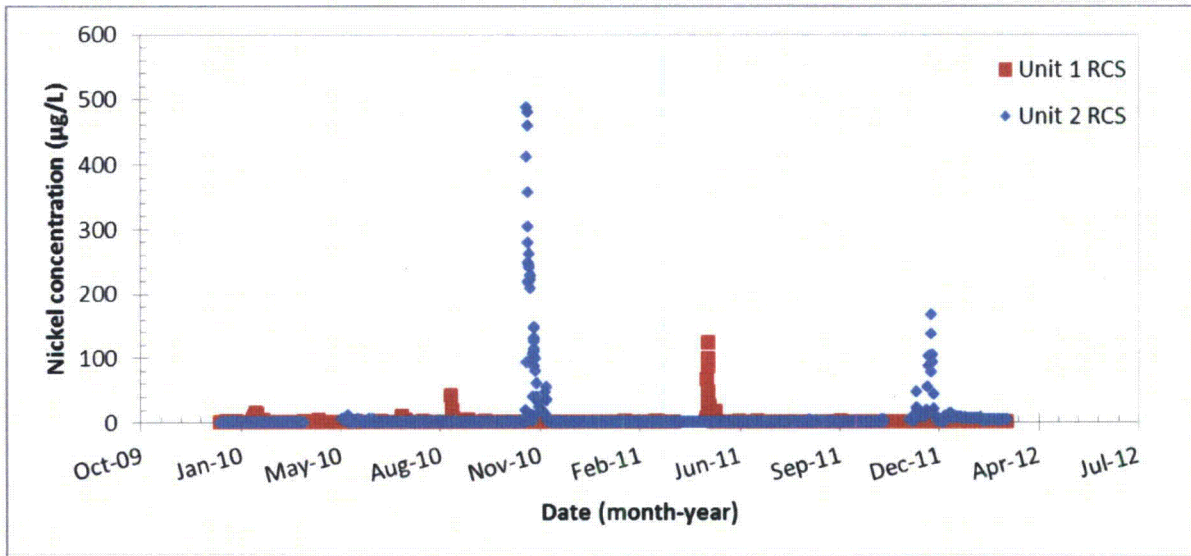


Figure 34: Nickel concentration in Unit 1 and Unit 2 RCS as a function of time.

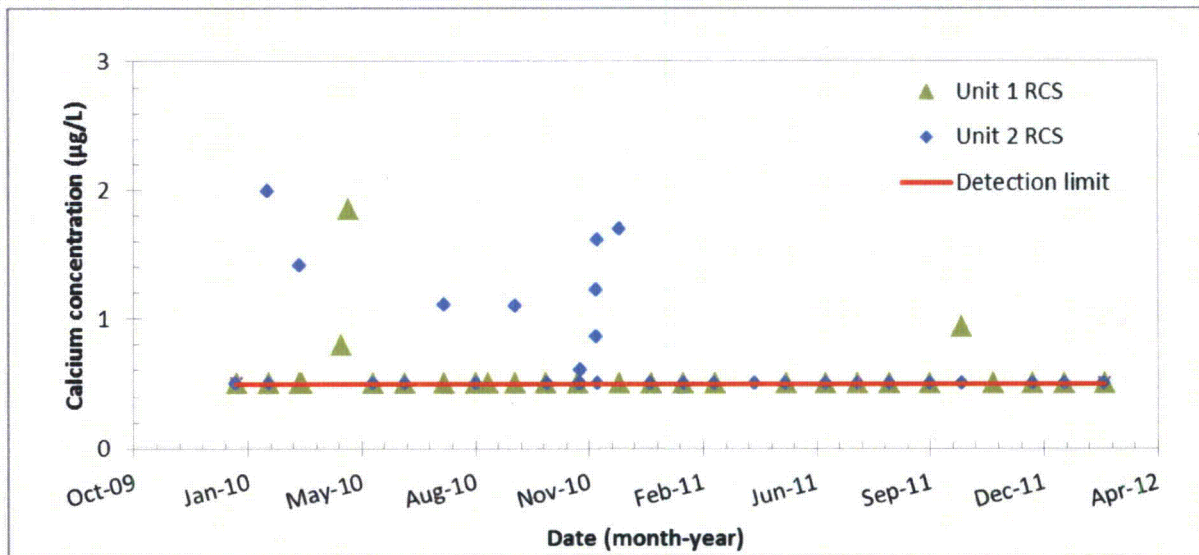


Figure 35: Calcium concentration in Unit 1 and Unit 2 RCS as a function of time.

RWST Related Graphs

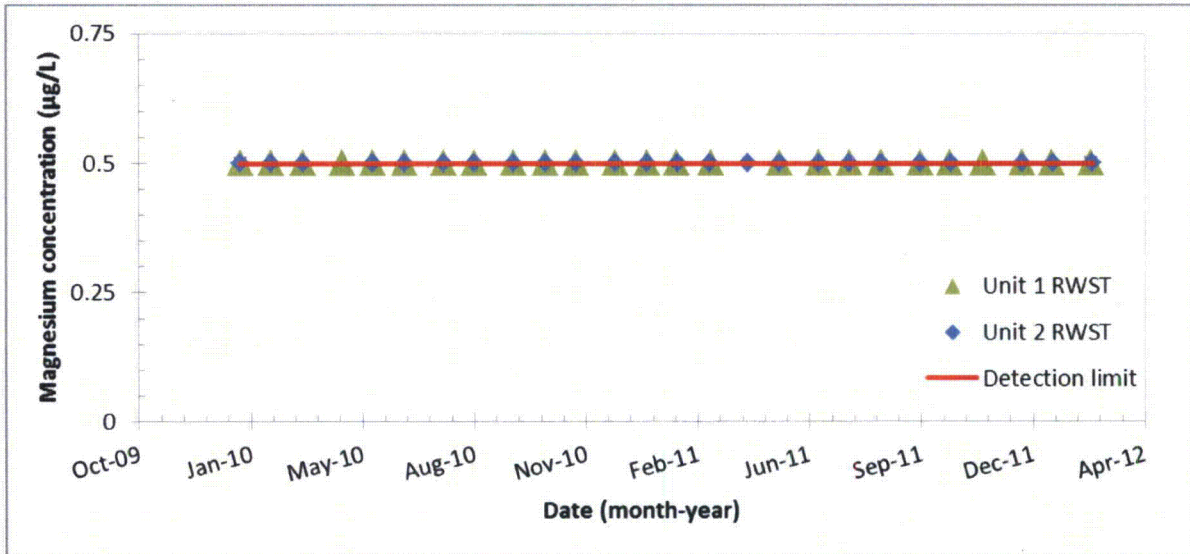


Figure 36: Magnesium concentration in Unit 1 and Unit 2 RWST as a function of time.

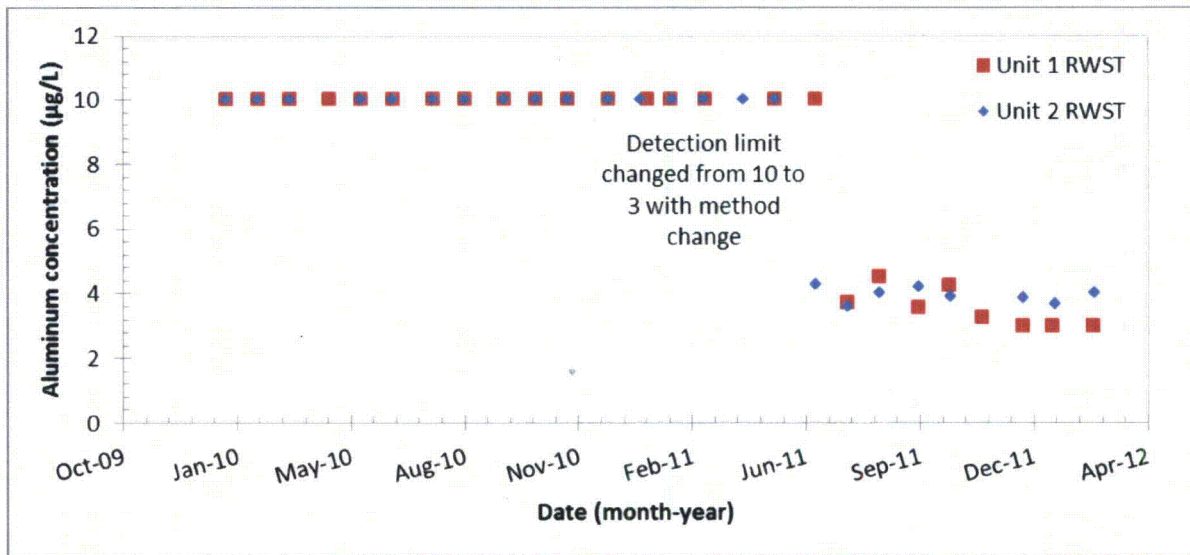


Figure 37: Aluminum concentration in Unit 1 and Unit 2 RWST as a function of time.

Title: Determination of the initial pool chemistry for the CHLE test

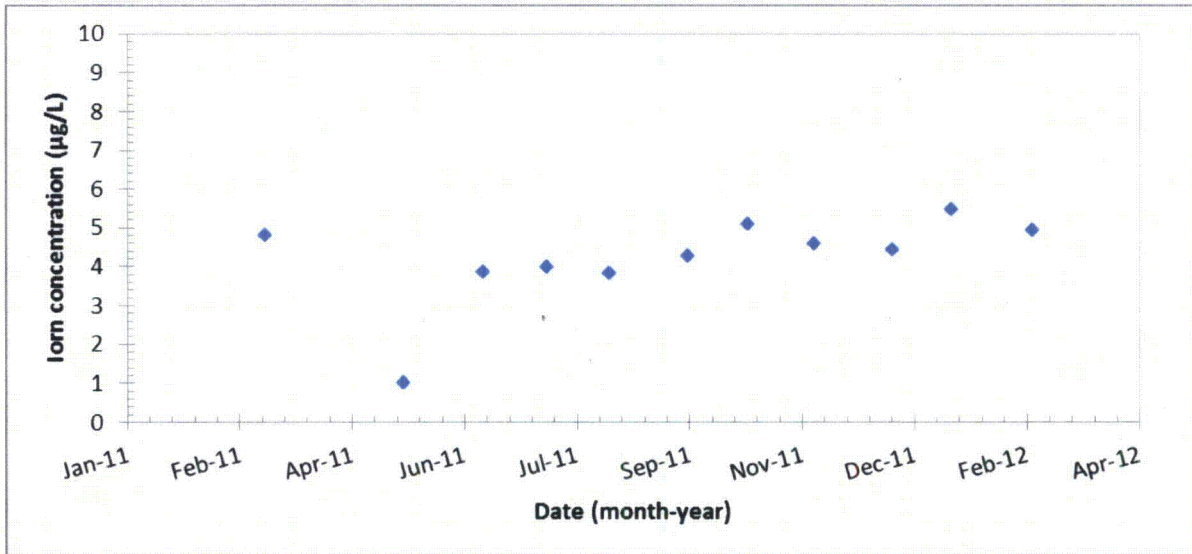


Figure 38: Iron concentration in Unit 1 RWST as a function of time.

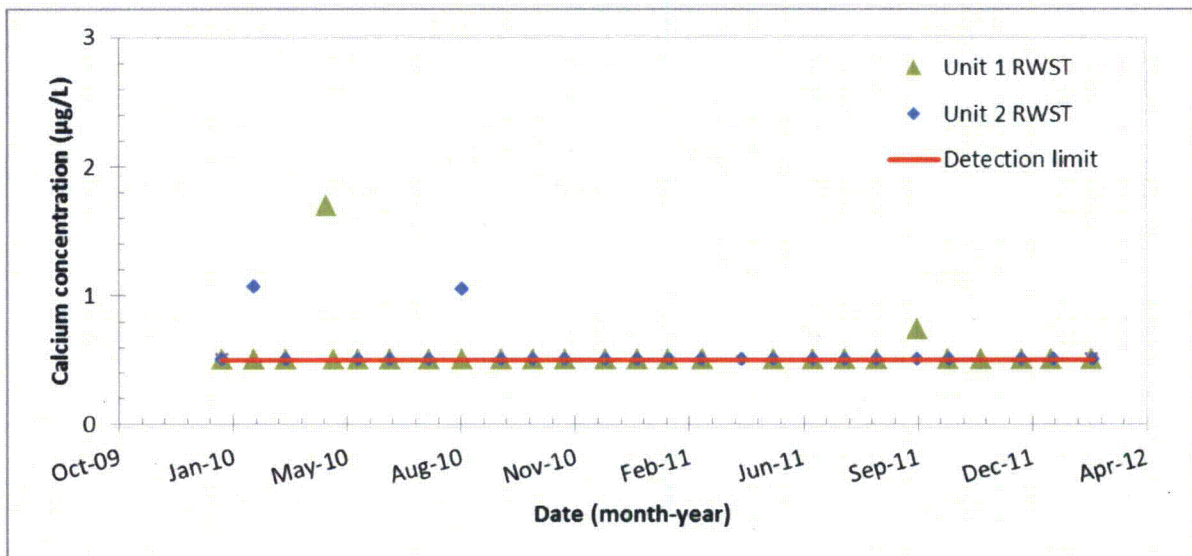


Figure 39: Calcium concentration in Unit 1 and Unit 2 RWST as a function of time.

### 3.8.1.1 Impurity Results

All impurities in both the RWST and RCS of both units were only detected in very small concentrations ( $\mu\text{g/L}$  or ppb levels), Figures 27-39; Therefore, they will be excluded from the chemical makeup of the initial pool concentration in the CHLE analyses.

## 3.9 Pool pH

The pool pH following a LOCA will vary due to the dissolution of TSP mass into the range boric acid concentrations in solution. For the STP design basis, using values (Table 3) for boric acid with the range

of TSP listed in Section 3.2 and solution volumes (Table 1), the pH during a LOCA will range 4.5 and will rise to a final pH of ~7.7 upon complete dissolution of TSP [5]. Using operational values for both solution volumes (Table 2) and boric acid concentrations (Table 18 and 19), with 15,100 lb of TSP, results in a smaller range of pH values as discussed below.

### 3.9.1 pH Analyses and Results

The pH range to be covered in the CHLE analyses was calculated from the operational values of the RCS, RWST, and accumulators for solution volumes (Table 2) and boric acid concentrations (Tables 18 and 19). These values, shown in Table 26, are calculated at 21 °C. This range of pH values (Table 26) only reflects the expected variance of the final pool pH. This range does not reflect the full pH profile expected as a result of a LOCA event; i.e. before, during, and after TSP dissolution into the pool. Therefore the median values for the steady state pH will be used in the CHLE tank test. The pH profile from dissolution of TSP into solution will be mimicked by pumping in a concentrated solution of TSP starting at 15 minutes after test initiation over a 65 minute duration as explained by sections 2.2 and 3.2. Therefore the test will have the lower pH approximately 4.5 (250 mM boron) and increase to approximately  $7.2 \pm 0.1$  over the first 80 minutes of testing.

Table 26: pH of the 30 Day test using the largest TSP concentration.

Statistical Parameter	pH
Median	7.17
Maximum	7.24
Minimum	7.09

Since TSP dissolution occurs within the first 1-2 hours of a 30 day test, it was decided to bound the minimum pH for bench tests through analysis of aluminum solubility characteristics as a function of pH as opposed to the initial pH of ~4.5, which rises quickly to the steady state pH during a LOCA. As seen in Figure 40, approximate minimum solubility of aluminum in borated buffered water ranges between 5.5 and 6.5 at the temperatures listed which encompasses the operational range of the tank test; therefore the average pH value of 6.0 will be the minimum pH in the bench test. The mid-point pH for the bench test will be the same as that used in the CHLE tank test, and the largest pH will be 7.7 as determined by conservative STP calculations [8].

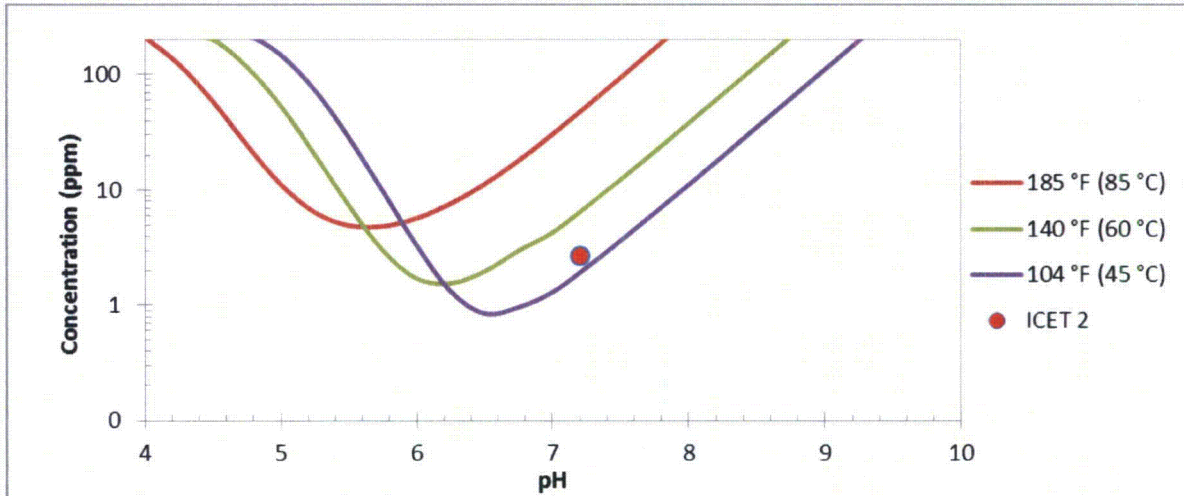


Figure 40: Aluminum solubility in borated buffered water.

### 3.10 Acid Generation Due to Irradiation

Strong acid is expected to form due to irradiation of containment following a LOCA. Nitric acid can form in response to irradiation of air and water. Hydrochloric acid may form due to irradiation or heating of electrical cable insulation [14]. The generation of these strong acids may result in a decrease of pool solution pH over time leading to the formation or increased formation of chemical precipitates of concern.

#### 3.10.1 Acid Generation Results

Calculations to determine the concentrations of strong acids following a LOCA at STP were previously performed [7]. It was determined that  $8.0 \times 10^{-4}$  M hydrochloric acid  $2.5 \times 10^{-4}$  M nitric acid would form over a thirty day period, Figure 41. The generation of both the hydrochloric and nitric acid is expected to decrease the pH by approximately 0.15 pH units over the same thirty day time period which can be seen in Figure 42.

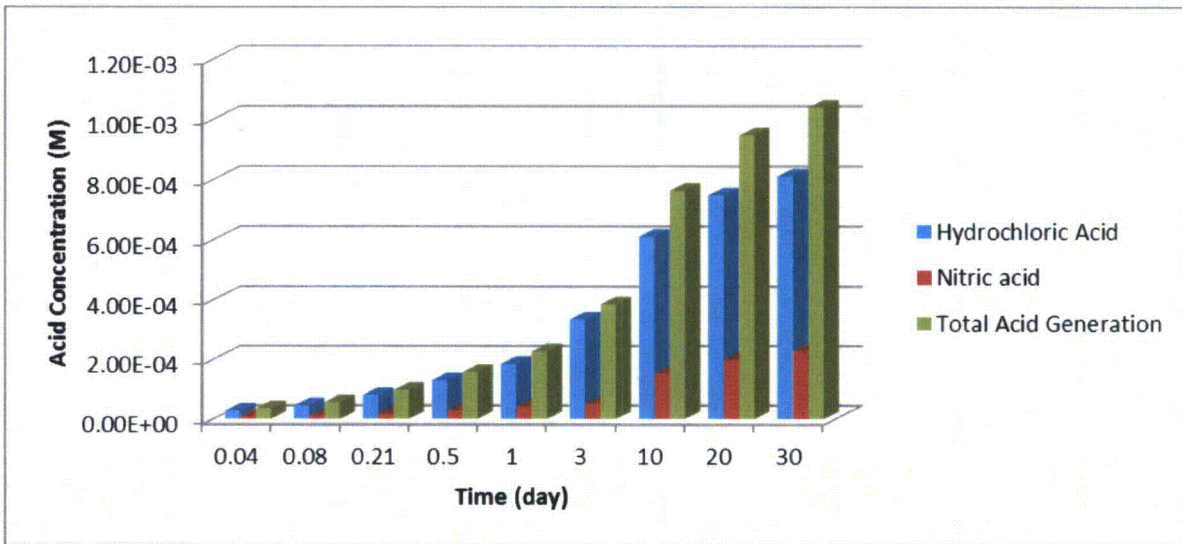


Figure 41: Generation of strong acid following a LOCA.

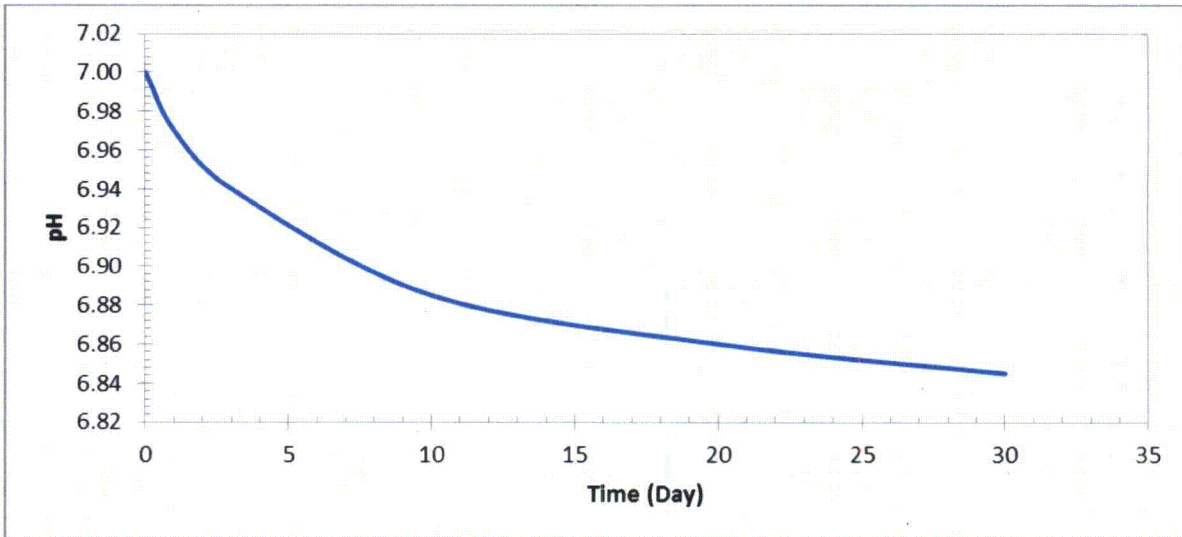


Figure 42: Decrease in pool solution pH as a result of acid generation, using an initial pH of 7 as a basis for comparison.

It is widely accepted that the solubility of the precipitates of concern, (i.e. aluminum hydroxide), is pH and temperature dependent. As shown by Figure 40, the post LOCA pool chemistry of ICET Test 2, which is similar to STP chemistry, results in solubility conditions near the minimum solubility concentration for the precipitates of concern. While a decrease of 0.15 pH units does not appear to be a significant change in solution pH, the temperature of the pool solution also decreases further reducing the solubility of possible precipitates.

### 3.10.2 Results

It was decided to add nitric and hydrochloric acid over time because the solution will be exposed to a chiller loop which may drop the temperature to or below the solubility limit of aluminum in solution. Therefore it is necessary to capture the possible effects of acid generation with temperature changes in the 30 Day test to fully evaluate the integrated chemical effects.

## 4 CHLE Pool Chemistry

The concentrations identified in Section 3 were multiplied by the 'best estimate' volume of corresponding solution to determine the pool chemistry of the CHLE test. A pH profile as detailed in sections 2.2 and 3.2 will be captured in the tank tests while a range of pH values will be captured in the the bench scale test. Table 27 contains a summary of chemical conditions to be captured by the CHLE tests. Table 28 list the acid to be added to the tank tests.

Table 27: Chemical conditions to be covered by the CHLE analyses.

Chemical	Bench Test Minimum (mg/L)	Bench Test Maximum (mg/L)	Tank Test (mg/L)
Boric Acid (Boron)	14,351 (2509)	16,918 (2958)	15,488 (2708)
Silicon	0.45	2.48	0
Lithium	N/A	N/A	0.42
TSP <sup>1</sup>	TBD	TBD	3,370
Final solution pH	6.0	7.7	7.2

<sup>1</sup> The concentration of TSP to be used in the bench test will be dictated by the boric acid concentrations and the target pH.

Table 28: Acid addition to CHLE test.

To be added	HNO <sub>3</sub> <sup>1</sup> (ml)	HCL <sup>2</sup> (ml)
24 hours	2.04	12.15
Day 3	2.84	14.05
Day 10	5.23	25.93
Day 20	3.30	12.92
Day 28	2.13	5.99

<sup>1</sup> Molarity of nitric acid is 15.7

<sup>2</sup> Molarity of hydrochloric acid is 12.1

## 5 Conclusion

In conclusion, these results were derived using a risk-informed approach. This approach provides a more accurate estimate of the chemical concentration than previous evaluations. The mass calculated from volumes and concentrations listed within this document will be used as design parameters for the CHLE analyses. The analysis of STP pool chemistry in this document is based on information that was

available at the time this document was prepared. Where final information was not available, values for chemical concentrations used in CHLE tests will be identified in the individual test plan documents.

## 6 References

1. Alion, *STP Post-LOCA Water Volume Analysis*, 2012, Alion Science and Technology: Albuquerque, NM.
2. Wheeler, R.E., *Quantile estimators of Johnson curve parameters*. *Biometrika*, 1980. 67(3): p. 725-728.
3. Conover, W.J., *Practical Nonparametric Statistics*. 1971, New York: John Wiley & Sons.
4. DeCoursey, W.J., *Statistics and Probability for Engineering Applications with Microsoft Excel*. 2003, MA: Elsevier Science.
5. STP, *TGX - Required Mass of TSP for LOCA Sump Solution pH Adjustment*, 2001, South Texas Project Nuclear Operating Company.
6. TAMU, *6" Cold Leg Break Simulation Results Sump Temperature = 200 – 150 °F*, 2012.
7. STP, *Post-LOCA Containment Sump pH and Maximum Iodine DF for AST Chapter 15 Analyses*, 2006, South Texas Project: Bay City, Texas.
8. STP, *MC-6480; MIN & MAX SUMP pH*, 1999, South Texas Project Nuclear Operating Company.
9. Rubin, K., J.L. Grover, and W.A. Henninger, *Spray Additive Elimination Analysis for the South Texas Project*, 1989: Pittsburgh, Pennsylvania.
10. STP, *Structural Reactor Containment Building TSP Baskets Fabrication and installation*, 2008, South Texas Project Nuclear Operating Company.
11. STP, *Condition Record 97-6223*, 1997, South Texas Project Nuclear Operating Company.
12. Wilkins, J.L., *TSP dissolution*, R.C. De Young, Editor 1973, Omaha Public Power.
13. Alion, *GSI-191 Containment Recirculation Sump Evaluation: CFD Transport Analysis, Revision 3*, October 21, 2008.
14. Beahm, E.C., R.A. Lorenz, and C.F. Weber, *Iodine Evolution and pH control*, 1992, Oak Ridge National Laboratory.
15. Chen, D., K.J. Howe, J. Dallman, and B.C. Letellier. "Corrosion of Aluminum in the Aqueous Chemical Environment of a Loss of Coolant Accident at a Nuclear Power Plant." *Corrosion Science*. Vol. 50, No. 4, pp. 1046-1057. 2008